IMPLICATIONS OF HYDROPOWER AND LAND USE CHANGE FOR ANTILLEAN MANATEES IN THE LOWER CHANGUINOLA RIVER, PANAMA: AN INTEGRATIVE MODELLING ANALYSIS

Victoria Reed, Department of Biology

McGill University, Montreal

May 29, 2017

A thesis submitted to McGill University in partial fulfillment of the requirements of the degree of Master of Science

TABLE OF CONTENTS

LIST OF TABLES

LIST OF FIGURES

APPENDICES TABLE AND FIGURES

ABSTRACT

Conservation of at-risk species is often threatened by development projects. This thesis focused on an endangered Antillean manatee (*Trichechus manatus manatus*) subpopulation in the lower Changuinola River (Bocas del Toro, Panama). This region has been reshaped by intensive agricultural activity and an upstream hydropower dam (Changuinola I). We hypothesized manatee feeding abundance and habitat suitability would be negatively affected by hydropower flow modification, and agricultural pollution would promote vegetation growth and manatee feeding. We built species distribution models using land use, environmental indicators and a hydrological model to estimate the effect of dam operations on the probability and abundance of manatee feeding. Our models indicated that mean weighted manatee feeding abundance decreased by 10.9% between February 2011 (before dam operation) and May 2015 (after dam operation). Water depth and land slope were the only significant predictors of both manatee feeding abundance and presence, and land use was only predictive in the presence/absence model. Combination of both models explained 34% of the variation in feeding, incorporating occurrence and abundance of feeding marks (r^2= 0.34). Our flow management strategy for Changuinola I showed that mean weighted manatee feeding abundance could only be marginally increased by 0.42% of 2015 levels, but monthly feeding variance reduced up to 2.63 times less than 2015 levels, even given the ideal management strategy maintaining a constant monthly discharge, while meeting target annual energy generation. Thus, hydropower flow management only has a slight effect on mean weighted feeding abundances, but a significant effect on foraging habitat stability.

RESUMÉ (FR)

La conservation des espèces en péril est souvent menacée par des projets de développement. Ce thèse se focus sur une sous-population du lamantin antillais (*Trichechus manatus manatus*) en danger dans la zone d'aval de la Changuinola (Bocas del Toro, Panama). Des activités agricoles intenses et un barrage hydroélectrique (Changuinola I) ont notablement remodelés cette région. Nous avons ému les hypothèses que la modification du débit hydroélectrique affecterait négativement le fourrage et l'habitat du lamantin et que la pollution agricole promouvrait la croissance de la végétation et le fourrage du lamantin. Nous avons construit des modèles de répartition des espèces en utilisant usage des sols, indicateurs environnementaux et un modèle hydrologique afin d'estimer l'effet des barrages sur la probabilité et l'abondance du fourrage du lamantin. Nos modèles ont indiqué que la moyenne pondérée de l'abondance du fourrage a diminué par 10.9% entre février 2011 (avant l'opération du barrage) et mai 2015 (après l'opération du barrage). Profondeur des eaux et la pente de terre représentaient les seuls prédicteurs significatifs de l'abondance et présence du lamantin et l'usage des sols n'était que prévisionnel dans la présence/l'absence du modèle. La combinaison des deux modèles expliquait 34% de la variation en fourrage, intégrant l'occurrence et l'abondance des traces alimentaires ($r^2 = 0.34$). Notre stratégie de gestion des flux pour le Changuinola I a démontré que la moyenne pondérée de l'abondance alimentaire au maximum peut augmenter par 0.42% de la valeur de 2015, mais la variance du fourrage mensuelle a été réduite jusqu'á 2.63 fois, étant donné que le décharge du Changuinola I est maintenu constant afin d'atteindre la production énergique annuelle ciblée. Ainsi la gestion

d’énergie hydraulique a seulement eu un effet modeste sur la moyenne pondérée de l’abondance alimentaire, mais un effet significatif sur la stabilité de l’habitat alimentaire.

ACKNOWLEDGEMENTS

This thesis would not have been possible without the support of several individuals. First and foremost, my supervisors, Brian Leung and Héctor Guzmán, for their continual guidance and input along the entire scientific process, from inception to project conclusion. Secondly, to my lab mates in both the Leung and Guzmán labs, your feedback, field assistance and senses of humour were invaluable (Catalina Gomez, Carlos Guevara, Javier Pinzón, David Ross, Emma Hudgins, Lidia Della Venezia, Andrew Sellers, Anthony Sardain, Natalie Richards, and Dat Nguyen). A special thank you goes to Alexis Montenegro, who captained our motorboat during the fieldwork data collection, and was instrumental in identifying both manatees, and manatee feeding marks at the site. Thanks also to Guillaume Larocque, Pablo Arroya, Jeffrey Cardille and Jacky Lee for their extraordinary expertise in GIS and remote sensing troubleshooting. To my supervisory committee members, Dr. Richard Condit and Dr. Raja Sengupta, for their insights and help framing the project scope and analyses. I would like to also thank the institutions that made this project possible with their generous financial sponsorship: McGill University, McGill Department of Biology, the McGill NEO program, the BESS CREATE grant/program, Québec Centre for Biodiversity Science, the Natural Sciences and Engineering Research Council of Canada, and AES Changuinola. I am very grateful as well to AES Changuinola, the Smithsonian Tropical Research Institute (STRI), and the Empresa de Transmisión Eléctrica, S. A. for both their invaluable databases, and (in the case of STRI) their laboratory facilities as well. Last, but certainly not least, to my family and friends for their continual support over the past 3 years, through the thick and thin.

CONTRIBUTION OF AUTHORS

I am the primary author of this thesis and, with guidance from Brian Leung and Héctor Guzmán, developed the scope and executed the methodology of this project. Héctor Guzmán, Catalina Gomez, Carlos Guevara, Javier Pinzón and Alexis Montenegro all assisted with field data collection, including: taking turbidity, salinity and depth measurements, as well as identifying manatee feeding marks. I conducted all data collection, parameterization of all models, and data analyses. Héctor Guzmán was involved in all project stages, from conception, contextualization, experimental design, analysis, and thesis revision. He was also the primary contact with AES Changuinola, an invaluable source of data with respect to their hydropower dam operations. Brian Leung was also involved in all project stages, from research proposal, to methodology, data analyses and final thesis revision. Leora Simon contributed to final thesis revision as well. Translation of the abstract into French was done by Anna-Lena Nadler.

PREFACE

This thesis seeks to bridge the fields of ecosystem-based management and biological conservation through the integration of interdisciplinary analysis techniques such as Geographic Information Systems (GIS), remote sensing, ecological modelling and fundamental hydrological concepts in an applied tropical biology context. We faced significant data limitations in this case study that required accommodations throughout the methodology. Though these accommodations are open to critique, they allowed analysis of a vulnerable system not uncommon to tropical or threatened species conservation and still provide a means of moving forward for research and management.

INTRODUCTION

Balancing societal needs with environmental and conservation objectives is a central objective of environmental management, but understanding their interactions is a challenge. Conservation managers must consider the need for efficient policy development, scientific analysis, and the preservation of societal needs versus ecological value. For example, a given natural resource, such as river flow, may be valued for its hydropower capabilities, but improper exploitation of this resource could undermine local species conservation efforts or affect other natural services provided by the river or habitat. To harmonize these competing interests, the field of ecosystem-based management has emerged.

Ecosystem-based management

Ecosystem-based management is the management of ecosystem health to conserve the environmental, economic and social benefits to society (Aswani et al., 2012). These benefits have been coined "ecosystem services" (Costanza & Daly, 1992; Gómez-Baggethun et al., 2010), and comprise the societal value gained from natural systems and their functions. Ecosystem-based management provides a structure to approach biological conservation from a holistic ecosystem-level perspective. This management scheme creates a resilient strategy to maintain place-based natural capital and services for present and future uses (McLeod et al., 2005).

The concept of ecosystem-based management is applicable across different industries, ecosystems and socio-economic strata. It has been widely developed in marine fisheries management practices (McLeod et al., 2005; Christie et al., 2007), and lauded as an alternative to the traditional top-down approach to conservation applied in both temperate and tropical regions (Aswani et al., 2012). The importance of integrating the ecosystem-based management framework with biodiversity conservation is far from a novel concept, but consensus on how best to incorporate the two is controversial (de Groot et al., 2010). Fortunately, however, conserving biodiversity frequently also preserves ecosystem services, such as eco-tourism, suggesting synergy between these objectives and a balancing of species' preservation with economic and social development (Egoh et al., 2009; Nelson et al., 2009; de Groot et al., 2010).

Priorities and challenges to conservation

The extent and severity of the current species' extinction crisis is widely debated, but it is undeniable that some species are more susceptible than others (Brooks et al., 2002). To maximize efficacy of mitigation strategies or policies, resource allocation to hotspot regions, vulnerable species and towards threats with the greatest impact is crucial (Mittermeier et al., 1998; Myers et al., 2000). There are 34 global biodiversity hotspots, predominantly in tropical climes, which have been reduced by 70% of their original land area (Mittermeier et al., 2004). Although many factors play a role in species' survival, a minimum of 75% of the terrestrial animal species classified as critically endangered, endangered, or vulnerable by the IUCN occur in areas experiencing significant habitat loss (Mittermeier et al., 1998). Thus, the regions of greatest concern (tropical ecosystem hotspots) are also the habitats of the most threatened species, where habitat loss is one of the greatest threats to survival (Marchese, 2015).

Often with less socio-economic means than their temperate counterparts, tropical countries face additional challenges to conservation, with natural resource extraction industries as the primary fuel for economic growth. Frequently, their economies are dependent on export-oriented industries, such as agriculture and fisheries, which can have a devastating impact on biodiversity (Lenzen et al., 2012), and lead to habitat degradation from pollution and over-harvesting (Tilman et al., 2001). Alongside this economic development is a rise in energy demand, often met in the form of hydroelectric power generation. Hydropower projects are growing in scale and number across the globe, (Ansar et al., 2014) resulting in a range of environmental and social implications from severe flow manipulation, flooding, community resettlement, deforestation, pollution from runoff, and fragmentation of habitats and migratory routes (Dudgeon, 2000; Malmqvist & Rundle, 2002; Nilsson et al., 2005). Hydropower development is innately dependent on running freshwater ecosystems, which are historically under-studied, despite their demonstrated heightened biodiversity loss (Ricciardi & Rasmussen, 1999; Malmqvist & Rundle, 2002; Dudgeon et al., 2006). In brief, tropical regions and freshwater systems are known harbours of biodiversity but concurrently exist in locales with exponential development, heightened habitat loss, limited data availability, and poorer socio-economic circumstances.

To overcome these conservation hurdles, tools such as traditional fieldwork, open source databases, Geographic Information Systems (GIS), and mathematical models can be combined to predict current, past and even future conditions. For instance, Species Distribution Models (SDMs) provide insight on the environmental variables that correlate with a species' occurrence (based on presence/absence survey data, or at minimum presence-only data). These habitat characteristics can take the form of remote sensing land use data (Kerr & Ostrovsky, 2003; Rushton et al., 2004; He et al., 2015), water quality parameters, and climatic or hydrological variables (Oberdorff et al., 2001; Buisson et al., 2008; Bond et al., 2011). Environmental variables are generally easier to measure or extrapolate from open source databases than species' occurrences. When it is not possible to directly observe a species in its habitat, proxies can be used for species' presence data. Proxies include scat, tracks (Hines et al., 2010; Karanth et al., 2011), browsing marks, and physical damage caused by trampling, grazing and browsing (Albon et al., 2007). While not exhaustive, these proxies capture areas critical to population conservation, such as foraging habitat (Lefebvre et al., 1999). The applications of this technique are promising for rare and vulnerable species with large or scattered ranges, such as *Panthera tigris* (tigers; Hines et al., 2010; Karanth et al., 2011), *Elephas maximus* (Asian elephants; Jathanna et al., 2015), or *Trichechus manatus* (West Indian manatees [Linnaeus, 1758]; Jiménez, 2005). Thus, presence proxies provide a means of applying SDMs to endangered species in data limited areas, such as tropical hotspots.

Our study focused on the endangered Antillean manatee (*Trichechus manatus manatus*), a subspecies of West Indian manatee, in the lower Changuinola River in Bocas del Toro, Panama. This case exemplifies numerous challenges facing conservation biologists working in tropical areas: a vulnerable species on the IUCN Red List (Deutsch et al., 2008; IUCN Species Survival Commission, 2000), limited species distribution data available for the lower Changuinola River, and challenging animal detection due to the environmental characteristics of the study site (Guzmán & Condit, in press). The objective of this study was to identify significant foraging habitat-determining characteristics of Antillean manatees in the lower Changuinola River, and thereby assimilate conservation of manatees into hydropower dam operations considering the natural flow of the channel system, Changuinola I operational capacity and the annual Changuinola I energy generation targets. This alternative flow management strategy allowed a comparison between the predicted natural flow prior to dam operation, 2015 Changuinola I modified flow, and future variance-reduced flow in the study site. We evaluated how Changuinola I is managed to meet its energy demands, the effects of flow modification on the downstream manatee foraging habitat in the lower Changuinola River, and how these might be modified to the greatest benefit for all. To address conservation concerns for the Antillean manatee, we integrated and applied a suite of management tools: species distribution modelling, remote sensing, foraging habitat proxies, fluvial geomorphology and management of hydropower generation.

METHODS

Study system

Trichechus manatus

There are two subspecies of West Indian manatee, one only found in Florida (*T. m. latirostris*, Florida manatee [Harlan,1824]), and the other in Central and northern South America (*T. m. manatus*, Antillean manatee); both are each listed as “endangered” and declining on the IUCN Red List (Deutsch et al., 2008). Latest population estimates place the Antillean manatee at only 6 700 individuals across its known range (Castelblanco-Martínez et al., 2012; Figure 1). The IUCN predicts a greater than 20% population decline over the next two generations due to current and predicted anthropogenic threats (Deutsch et al., 2008).

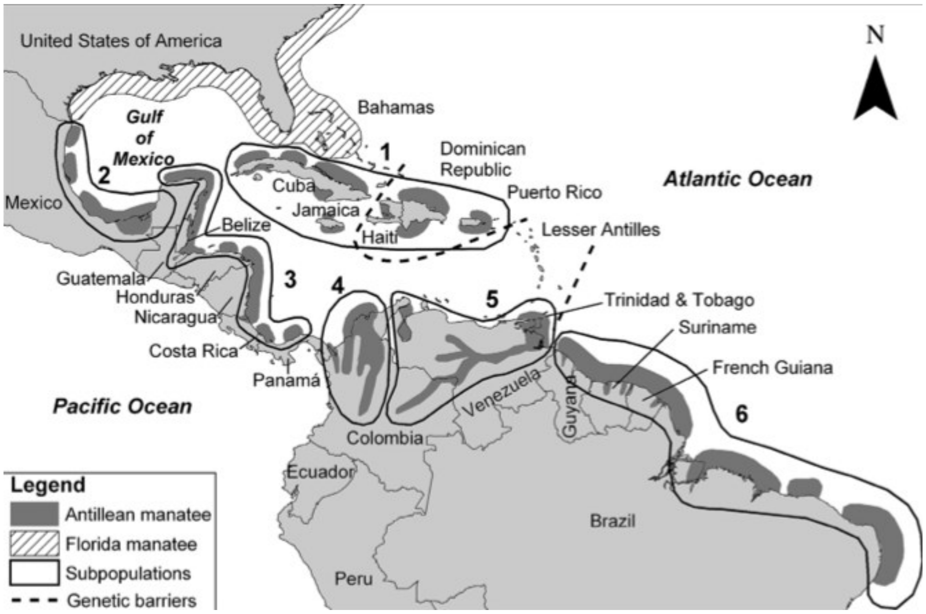

Figure 1 Population distribution of *T. m. latirostris* and *T. m. manatus* in North and South America. Dark grey shading indicates the Antillean manatee range, hatches the Florida manatee range, and the solid lines represent subpopulations and the dashed lines are areas of likely genetic barriers (Castelblanco-Martínez et al., 2012).

Panama

The main Antillean manatee population in Panama can be found in Bocas del Toro province, (Mou Sue et al., 1990; Guzmán & Rivera-Chavarria, 2014; Guzmán & Condit, in press) in the San San Pond Sack Wetlands protected area (Quintana-Rizzo & Reynolds, 2010; Figure 2). The population between 1987 and 2013 appears to have remained stable, ranging from 42-72 manatees in 1987, determined by aerial survey data (Mou Sue et al., 1990), to 33 individuals at peak season in May 2013 according to Bayesian modeling and side-scan sonar estimates (Guzmán & Condit, in press). However, with such a small population, the Panamanian population is vulnerable to extirpation, while also providing a potentially critical bridge between South and Central American manatee subpopulations (Castelblanco-Martínez et al., 2012; Díaz-Ferguson et al., in press). Turbid and thickly vegetated waterways make species detection challenging in the Changuinola River, far more so than the neighbouring San San River (Mou Sue et al., 1990; Guzmán & Condit, in press). As a result, it is unclear what attracts manatees to the Changuinola River and identifying these characteristics is important for species and habitat conservation (Gonzalez-Socoloske et al., 2015).

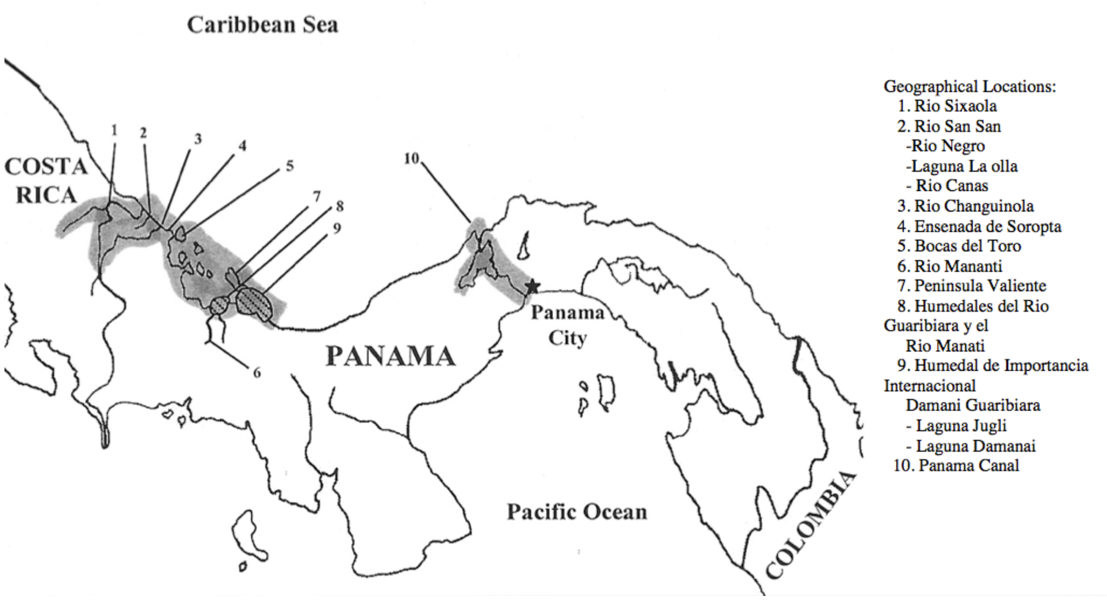

Figure 2 Population distribution of *T. m. manatus* in Panama. Grey shading highlights the watersheds with manatees present (Quintana-Rizzo & Reynolds, 2010).

Manatee habitat characteristics

Temperature, waterway depth and width, salinity, currents, forest cover, abundance of aquatic vegetation and motorboat traffic have been identified as habitat-limiting factors for West Indian manatees (Jiménez, 2005; LaCommare et al., 2008). In general, wide, secluded and warm water bodies with low flow rates, shallow depths, with a variety of vegetation typify manatee habitat. They can tolerate salinity levels that range from fresh to salt water.

Temperature sensitivity is generally only a reported issue for Florida manatees, given seasonal fluctuations in northern latitudes (Smith, 1993; Deutsch et al., 2008). Each of these factors have been investigated in some capacity, although some of the evidence has only been described anecdotally; the level of importance of each factor has yet to be investigated in the lower Changuinola River. Our analysis integrates the western Panamanian manatee population into the broader context of West Indian manatee habitat research.

Threats to conservation

Characterized by a long lifespan and slow reproductive rate, West Indian manatees are highly susceptible to environmental changes and pressures (Quintana-Rizzo & Reynolds, 2010). Habitat variables are the most significant predictors of manatee presence, with much greater influence than inter or intra-specific competition or predation (Quintana-Rizzo & Reynolds, 2010). Habitat loss is considered one of the most significant threats facing Sirenians (manatees and dugongs) (Marsh et al., 1986; Castelblanco-Martínez et al., 2012). The plethora of threats (i.e. hunting, urban development, agricultural and industrial runoff, and hydroelectric expansion), combined with their slow breeding cycle and minimal genetic variation within and between populations, contributes to the manatees' vulnerability in Panama and across its range (Hunter et al., 2010; Castelblanco-Martínez et al., 2012; Díaz-Ferguson et al., in press; Guzmán & Condit, in press).

Panama

Poaching, agro-chemical pollution and motorboat traffic threaten manatee conservation in Bocas del Toro, particularly with motorboat noise pollution interrupting mother-calf communication (Mou Sue et al., 1990; Quintana-Rizzo & Reynolds, 2010; Guzmán & Rivera-

Chavarria, 2014). The expansion of banana agriculture during the 20^{th} century was characterised by intensified applications of pesticides, fungicides, and fertilizers to combat the increasingly resistant agricultural pests and degrading soil conditions. Direct wastewater discharge and widespread deforestation caused by the development of these, cattle, and teak plantations have resulted in heavy metal pollution, nutrification and sedimentation in local waterways and receiving bays (Guzmán & Jiménez, 1992; Collin, 2005; D'Croz et al., 2005; Seemann et al., 2014). Furthermore, river fragmentation and flow alterations from recent hydropower development have the potential to reduce habitat persistence (Freeman et al., 2001). With its longstanding effects on flow regulation, overall habitat preservation, and detriment for aquatic biodiversity, the scope of this study was narrowed to hydropower development and changes in surrounding land use.

In 2011, AES Changuinola began operation of the 223MW Changuinola I dam after four years of construction inside the Bosque Proyector de Palo Seco protected forest area in Bocas del Toro, Panama (AES Changuinola, 2013). Located downstream from this dam, in a system of interconnected artificial irrigation and navigation channels on the lower Changuinola River, is a subpopulation of Antillean manatees (Mou Sue et al., 1990; Guzmán & Rivera-Chavarria, 2014; Guzmán & Condit, in press). With uncertainty surrounding the population status of these manatees in the lower Changuinola River, we developed a methodology that incorporated fieldwork, remote sensing, foraging habitat proxies, fluvial geomorphology and species distribution modelling to elucidate the potential implications of hydropower activities and land use change on this vulnerable species.

Changuinola River

The study focus area is the downstream region of the Changuinola River (9°27’49”N, 82°26’36”W). With an entire watershed area of 3202km^2, it is characterized by relatively low uniform elevation near the river mouth (less than 20m above sea level), turbid waters, and high levels of floating aquatic vegetation which both impede water visibility and maneuverability (Mou Sue et al., 1990; Empresa de Transmisión Eléctrica, S. A. [ETESA], 2009; Guzmán & Rivera-Chavarria, 2014). Water temperatures downstream do not drop below 20°C, a critical threshold for manatees (Deutsch et al., 2008; unpublished HOBO data, 2015-2016). The area is a humid tropical climate; the seasonal variations in precipitation are characterized by “dry” periods, generally between January and April, and “wet” season for the remainder of the year (D’Croz et al., 2005). Mean annual rainfall in Changuinola town is approximately 2615mm (Kaufmann & Thompson, 2005) and the tidal variation does not exceed 0.5m (Guzmán et al., 2005).

Navigation and irrigation channels built by banana corporations in the early 20th century were used by manatees in the late 1980s, (Mou Sue et al., 1990, Cramer, 2013), and present day use was confirmed during our field surveys. This artificial canal system is not static, with regular inundations in the area tending to clear away the thickets of floating aquatic vegetation that densely cover them in the dry season (H. Guzmán, personal communication, Sept. 28, 2016). A significant flooding event in May 2005 (ETESA, 2008) caused a permanent change to the mouth of the Changuinola River by inundating a section of one of the western channels, and creating a large lagoon now also an observed feeding area for manatees.

Field data collection

We collected all field data between April 29 and May 2, 2016, at the end of the dry season in Panama. This is when the water depth was predicted to be at its (approximate) lowest, and thus was selected to illustrate the most limited channel accessibility that the manatees experience throughout the year. Navigability constraints defined the perimeter of the study site, as we were unable to traverse the most densely vegetated channels. The study site represents the lower 27km^2 area of the Changuinola River and neighbouring artificial channels, within the first 4km of the main stem, to the upper limit where manatee feeding marks have been observed (Figure 3).

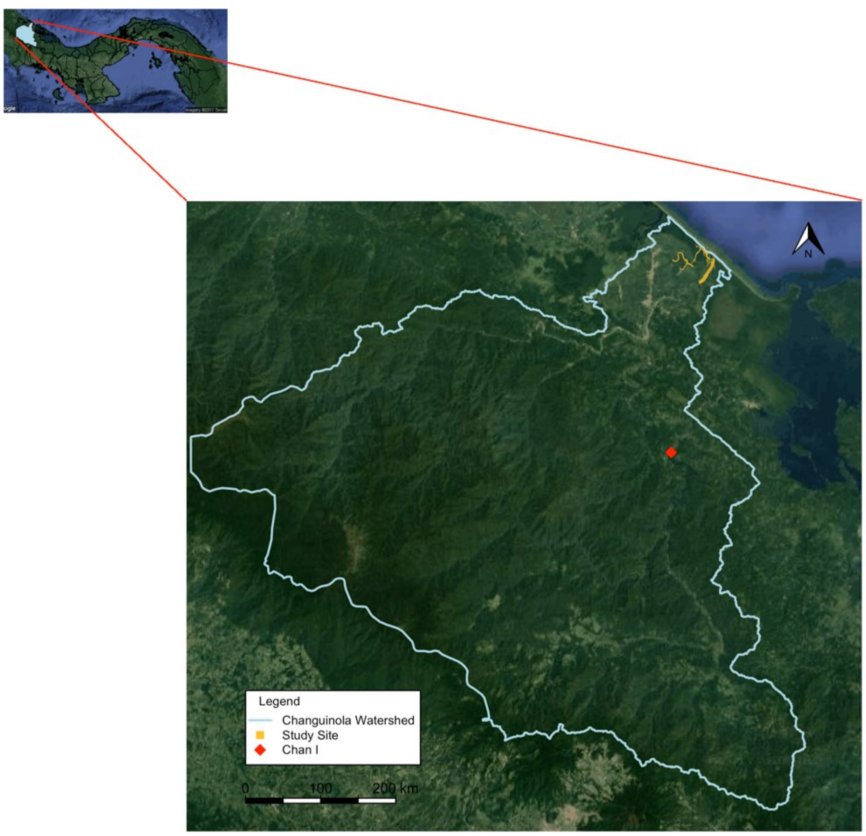

Figure 3 Changuinola watershed (blue) in Bocas del Toro, Panama (STRI, 2013), the study site where all field data was collected (orange), and the Changuinola I dam (red diamond).

Depth profile

We generated the depth profile of the lagoon system using a Hummingbird 385ci Global Positioning System (GPS) fishfinder (WGS84) secured to the back of a motorboat. Travelling at 4km/h, we drove the motorboat in a zigzag pattern across all accessible lagoons and channels in the lower reaches of the Changuinola River. We took depth measurements once every five seconds in most areas, unless the areas were very constricted by aquatic vegetation, in which case the measurement frequency was increased to once every second.

Salinity

We collected salinity measurements using a Vee Gee STX-3 Salinity Scale Optical Refractometer throughout the lower Changuinola River, irrigation channels and lagoon. We selected sampling points based on microhabitat characteristics (e.g. different water colours, different points within a channel, and varying distances from the mouth of the river). We took two salinity measurements at each point; one at the surface of the water, and another to the nearest half meter of the actual water depth (e.g. if the water was 2m deep, a sample was taken at about 1.5m depth). Because no surface water sample yielded a salinity value greater than 0, only the deep salinity samples were used in the analysis. We took a GPS coordinate (WGS84) at each location, with a GPS accurate to within 2m.

Turbidity

We measured turbidity using an EISCO limnological turbidity tube with Secchi disk at the same locations where salinity measurements were taken. These samples were taken at the surface, with total depth and time of sample also recorded. We filled the tube with water and slowly released it from a valve at the base until the black and white target disk became visible.

At this point, a measurement was taken in centimeters. To convert these distance values into Nephelometric Turbidity Units (NTU), we used the following equation:

Equation 1

$$\text{Depth in Centimetres} = 244.13 * (\text{Turbidity in NTU})^{-0.662}$$

(State of Utah Department of Environmental Quality, 2014)

Vegetation feeding survey

West Indian manatees spend 6-8 hours per day feeding, and thus their feeding marks were used as a proxy for species' presence and foraging habitat (Hartman, 1979; Jiménez, 2005). We drove a motorboat at 4km/h on both banks of the lower Changuinola River and along all navigable channels to record all feeding marks on bank and surface vegetation. A local boatman assisted us with common plant and mark identification. At any one time, there were a minimum of three people scanning the vegetation for feeding marks. Marks were identifiable by the characteristic jagged appearance of manatee bite marks (very different from machete or motorboat propeller marks, which produce uniform and straight cuts on the vegetation; Jiménez, 2005). Underwater vegetation was not plausible to survey, given the poor water clarity. Waypoint numbers were recorded at each feeding location observed, with a GPS accuracy of 2m (WGS84). Please note that the term "feeding abundance" refers to feeding marks per square meter as a measure of manatee feeding mark density.

Landsat classification

We classified a selection of Landsat images to determine the land use in the study area. This classification step allowed the integration of land cover classification into the SDMs developed.

Image selection

We selected Landsat images from the USGS Earth Explorer database that covered the Changuinola River watershed, including the lagoon and channels near the mouth of the Changuinola River (for coordinates, see Appendix, Table A1). We reviewed satellite imagery over a 15-year period (2000-2015) to identify images in the region with less than 20% cloud cover (a prevalent issue in tropical remote sensing optical imagery). Images taken by Landsat 7 after May 2003 have missing data bands, which caused an additional complication to identify images with sufficient data in the study region (USGS, 2015). These combined challenges resulted in the selection of seven Landsat images from Landsat satellites 5, 7, and 8 over the 15 years (see Appendix, Table A2), and one global land classification (GlobCover 2009), to fill-in any remaining missing data gaps in the optical imagery.

Image pre-processing

All images across all years were pre-processed in ENVI 5.3. We created a cloud mask and applied it using MATLAB (Zhu & Woodcock 2012; Zhu et al., 2015). Once all the cloud masks were created, we radiometrically calibrated the images using the settings appropriate to Fast Line-of-sight Atmospheric Analysis of Hypercubes (FLAASH) preparation, and subsequently atmospherically corrected them using the FLAASH tool. We ran a range of different FLAASH models on each image, and selected and compared the spectral profiles of 4 regions of interest in water, vegetation and soil classes to estimate the accuracy of the atmospheric correction. The optimal atmospherically corrected image was selected based on the closest representation of each class' spectral signature and values (Bowker et al., 1985). Once the pre-processed and atmospherically corrected image was selected, we applied the cloud mask created in MATLAB (see Appendix for full details on the pre-processing procedure).

Image classification

Six land use classes were defined: forest, non-forest vegetation, agriculture, water, soil (exposed land) and urban cover based on the class delineations given by Hopkins II (2009) and Sliva & Williams (2001). Broad land use classes are appropriate for habitat, riparian and land use analyses (Johnson et al., 1997). Soil, or exposed land, was included (as in Hopkins II (2009)) to indicate high erosion and runoff-susceptible areas. We applied maximum likelihood supervised classification to all images due to its class precision (classifications were compared to higher resolution Google Earth imagery, and pixel spectral profiles) and time efficiency. A minimum of 1000 training pixels were used in each image for each class (See Appendix, Table A3). We manually varied the weighting of each class to compensate for cases where classes exhibit similar spectral profiles (e.g. forest and non-forest vegetation; see Appendix for an example of spectral signatures; Figure A1).

Filling in data gaps

We processed classified images in Google Earth Engine using the Bayesian Updating of Land Cover Classification (BULC) algorithm. BULC fills data gaps by determining the agreement between land cover classifications from year to year and estimating the most likely land class at a given pixel (see Cardille & Fortin, 2016 for full algorithm details). This algorithm requires one complete base layer without missing pixel values, so we inputted GlobCover 2009 as the base layer (ESA, 2010). We reclassified the 23 classes of GlobCover 2009 into the 6 classes identified in this study using the remap function in Google Earth Engine (see Appendix, Table A4 for details). We ran the BULC script in the Code Editor of Google Earth Engine and produced 7 complete land cover classification maps. We used the final May 2015 classification map in the SDMs developed in the next section, ultimately with less than 2% of the pixel values needed from GlobCover 2009. The final February 2011 classification map was used in the backcasting scenario, as representative of "pre-dam" operation conditions. Thus, the final 2015 classification image was a result of seven BULC-integrated Landsat images and GlobCover 2009 data, and the final 2011 classification image was a result of six BULC-integrated Landsat images and GlobCover 2009 data. The proportions of each land use class were extracted from each year within a 5km radius of the study site to compare pre/post dam operation.

Species distribution model

We discretized the lower Changuinola River and surrounding channels and lagoon in ArcGIS 10.3 into 626 ($100m^2$) grid cells, each containing information on local environmental variables. We applied a spline function to the collected salinity, depth, and turbidity values using QGIS and GRASS software version 2.14.3 to interpolate the values for each of these variables within all grid cells. We calculated the width of the river and the lagoons using the Near function and shoreline points created along the river and channel banks within ArcGIS 10.3. We applied the Spline function in ArcGIS 10.3 to the SRTM void-filled HydroSHEDS 90m Digital Elevation Model (DEM) to calculate the slope. To associate land use classes to each grid cell, we extracted the proportion of each land use class around each grid cell by applying buffers of varying radii. The proportions of all land use classes (excluding water, as this is a pre-requisite for all manatee presences), were inputted as predictor variables in the SDM. The buffer radii were optimized using the optim function in R Studio 3.3 to select for the highest adjusted r-squared value obtained in every SDM run for each land use class and corresponding buffer radius (Wood, 2016). Land use class proportions were extracted from both the February 2011 and May 2015 land use maps, with the model fit to May 2015 data and buffer radii. February 2011 land use class proportions were used for the backcasting scenario.

Development of SDM (2015 Model)

We used a Generalized Additive Model (GAM) as the base of our SDMs to determine the relationship between the environmental variables described above (depth, salinity, turbidity, waterway width, slope, and surrounding land types) and foraging habitat (the occurrence and abundance of feeding marks). We ran three analyses to generate our predictions. First, we modelled the presence-absence of feeding marks in each of the 626 grid cells versus the environmental predictors (PA model). Second, we modelled the feeding abundance per unit area of each grid cell only where feeding marks were recorded (FA model). In the third analysis, we combined both models by multiplying the output of the PA and FA model (yielding the combined model), which provided the expected feeding marks per unit area of each grid cell. This approach was modelled after the method applied by Barry & Welsh (2002) to accommodate for zero-inflated data in SDMs. We ran the SDMs in R-Studio 3.3 using the mgcv package (Wood, 2016). We determined the fit of the PA, FA and combined models by calculating the ordinary least squares regression, r^2, of the models ran with only significant variables.

Linking hydropower management with manatee foraging habitat

The consequences of hydropower development on manatee conservation was a central focus of this thesis. This required the integration of three components: a flow accumulation grid to estimate natural watershed flow, a means of estimating downstream discharge, and a relationship between downstream discharge and river depth at the study site. To generate a flow accumulation grid from the same SRTM 90m resolution DEM used to calculate slope, DEM depressions were filled by identifying sinks using the method outlined by the Environmental Systems Research Institute ([ESRI], 2016). Once completed, the flow accumulation grid was created using the output from the Flow Direction tool, and clipped to the area of the Changuinola watershed. Flow accumulation, as a measurement of the number of upstream cells that flow into a given cell, is also an approximation of basin area, and was used to estimate proportional flow in the watershed (Das & Paul, 2006).

To predict mean flow at the site at the time of sampling in May 2015, we used empirical flow data from three ETESA sites (910102, 910202, and 910401) and the Changuinola I dam (in 2015), and flow accumulation estimates (Figure 4). Data for each ETESA station ranged between January 1st 2000- July 18th 2013, January 1st 2000- April 30 2012, and June 12th 2001- November 11th 2002, respectively. In cases where data gaps existed in the gauge discharge data, the na.interp function in the forecast package of R was used to interpolate these values (Moritz et al., 2015). Once full flow datasets were created, we determined the mean monthly flow across a typical year at each of the three ETESA gauges prior to 2011 (before the Changuinola dam began operation). It was important to estimate these values prior to 2011 to relate empirical flow estimates to the flow accumulation grid.

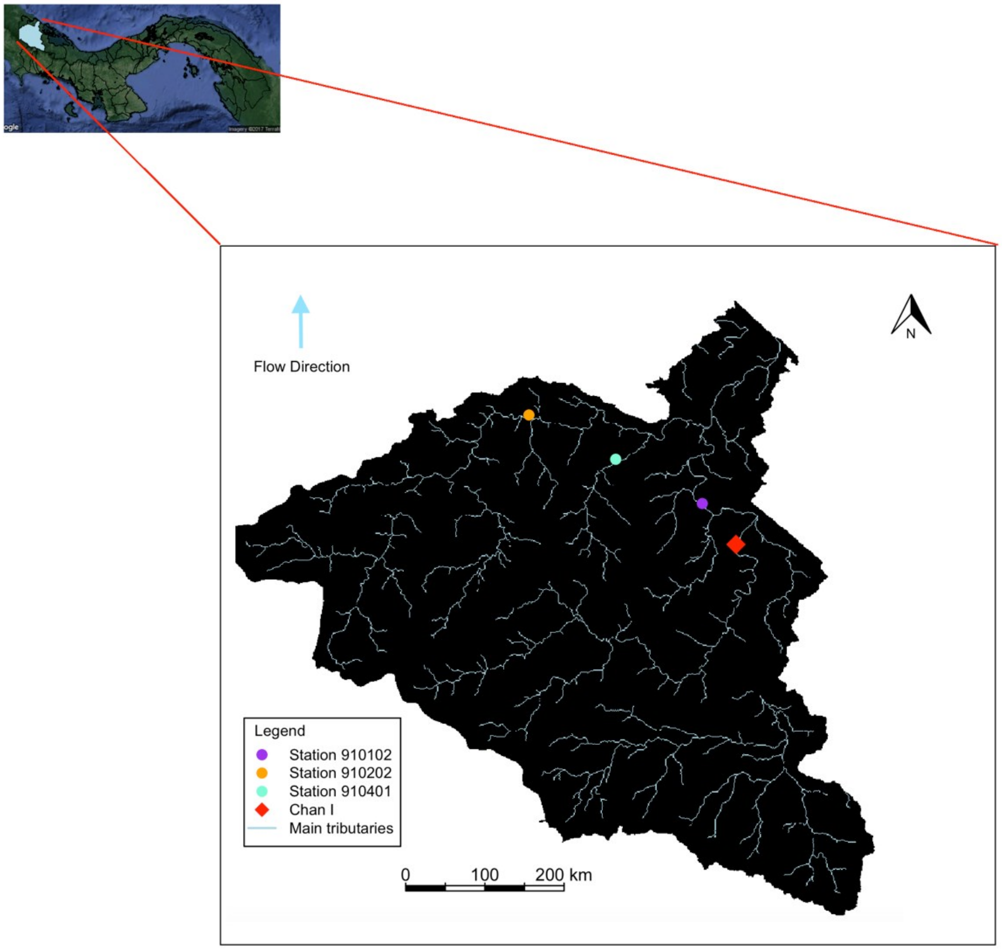

Figure 4 Map of the Changuinola watershed in Bocas del Toro province, Panama (STRI, 2013), the three ETESA discharge gauges used to build our hydrological model (latest discharge data collected on January 16, 2017; ETESA, n.d.), and the Changuinola I dam (red diamond). River discharge flows northward.

With the flow accumulation grid developed, the relationship between the standardized monthly ETESA gauge discharge values and the standardized extrapolated flow accumulation values at each gauge were linearly regressed on a 1:1 line (where each monthly gauge value was divided by the maximum discharge for that given month across all stations, and all flow accumulation values were divided by the maximum gauge flow accumulation). The strength of this linear relationship confirmed whether flow accumulation, and the proportional relationship between flow accumulation values at the gauges, could be used as a proxy to estimate natural flows (Das & Paul, 2006; Kuemmerlen et al., 2014). The regression line fit to this relationship was used to estimate what the natural flow at the Changuinola I dam would have been (per the flow accumulation at its location), had the dam not been built (represented by Q_{nat} in Equation 3). With the assumption that this linear relationship between discharge rate and flow accumulation holds across the watershed, the flow unaccounted for by the three gauges was estimated as a fraction of the total natural flow between stations 910102, 910401, and 910202. With these proportions of flow accumulation, we developed the following equation to estimate downstream mean flow at the site for a given month, without (Equation 2) and with (Equation 3) the dam present:

Equation 2

$$Q_{site} = (1 + p_1) * (Q_{910102} + Q_{910401} + Q_{910202})$$

Equation 3

$$Q_{site} = (1 + p_1) * (Q_{910102} + Q_{910401} + Q_{910202}) - Q_{nat} + Q_{chan}$$

Where Q_{910102}, Q_{910401}, and Q_{910202} are the monthly flow values (m^3/s) at a given gauge, Q_{site} is the monthly flow at the study site (m^3/s), Q_{nat} is the estimated expected monthly natural flow at the dam location prior to its operation calculated using the regression of flow accumulation versus discharge rate above (m^3/s), Q_{chan} is the mean monthly flow released through the Changuinola I dam in 2015 (m^3/s), and p_1 is the proportional flow accumulation of cells unaccounted for by the ETESA gauges. Note that only the discharge values from the three ETESA gauges prior to 2011 were used to estimate natural flow (both for ungauged channels and estimated natural flow at the Changuinola I dam location). Q_{chan} was entirely based on discharge data (total dam releases including turbine and base ecological flow) provided by AES Changuinola for the year 2015 (AES Changuinola, personal communication, Mar. 21, 2016). There are three ETESA precipitation gauges in the Changuinola watershed, but one only collected data between May 27th and October 31st 2015. To determine if a precipitation factor should be incorporated into the model, we applied a paired t-test to compare mean annual precipitation values for the remaining two ETESA stations (91001 and 91030) for the complete overlapping years: between 2006 and 2015, excluding 2012 which was not recorded at station 91030. We did not incorporate precipitation into the model because the null hypothesis that mean annual precipitation between the two stations was the same could not be rejected (paired t-test, $p = 0.1831$), and even if this value were significant, there was not sufficient data at only two stations to parameterize precipitation into the model. Thus, we considered the mean discharge rates sufficient to estimate natural flow.

To link hydropower operation with the SDMs, we related river flow with river depth downstream. This relationship is described as the river continuity relation in fluvial geomorphology:

Equation 4

$$Q = w*d*v$$

Where Q is discharge (m^3/s), w is channel width (m), d is average depth of channel (m), and v is mean velocity (m/s) (Leopold & Maddock, 1953; Hickin, 1995). To estimate velocity, Manning's equation was applied:

Equation 5

$$v = (n^{-1})*(R^{2/3})*(S^{1/2});$$

Where n is Manning's roughness coefficient (or coefficient of roughness, a value which estimates the coarseness of the riverbed), R is the hydraulic radius (m, calculated by dividing the cross-sectional area by perimeter), and S is the channel slope (m/m). A first order approximation was applied to relate upstream discharge rate to the downstream depth values. First, the channel width is assumed to remain constant with changing flow, and the bankfull channel is assumed to have a rectangular cross-section with a flat river bed and vertical banks, as would be the case in a one-dimensional impervious channel (Julien, 2002). Second, with the mean channel width more than 120 times larger than the mean depth, the wetted perimeter (P) and hydraulic radius (R) could be estimated as (Julien, 2002):

$P \cong w;$ therefore,

$R \cong d;$

In the case of these assumptions, we can simplify equations 4 and 5 into a singular constant variable, K, as follows:

Equation 6

$$Q = w*(S^{1/2})*d*d^{2/3};$$

$$Q = w*(n^{-1})(S^{1/2})*(d^{5/3});$$

With $w*(n^{-1})(S^{1/2})$ as a constant (K);

Equation 7

$$Q = K*(d^{5/3})$$

This relation is a derivative of the integration of Manning's equation and the continuity relation, and it is generally accepted that most river flows exhibit this relation (Julien, 2002). Thus, with a prediction of mean flow at the study site at the time of sampling, and the mean depth measured, a constant value of K was calculated and was used in Equation 7 for our predictions.

The 2015 discharge values provided by AES Changuinola were used to determine the Q_{chan} value in Equation 3, to solve for the mean discharge rate in the manatee habitat at the lower Changuinola River (Q_{site}) in May. Q_{site} was incorporated into Equation 7, along with the mean depth value from the site depth spline interpolation map, to calculate the constant K value. With this K value and Equation 7, mean depth could be estimated for any given mean discharge value. The differences between the calculated mean depth and the real measured site mean depth (residuals) were recorded, allowing variation in local depths across grid cells. To backcast into February 2011 (the date of the satellite image from 2011), the estimated mean February monthly flow for 2011 using Equation 2, and the residual differences between local depth and mean depth from Equation 7, were used to predict the channel depth changes at each grid cell. These depths, and the extracted land use class proportions, were then used to predict foraging habitat in 2011.

Alternative management strategy

Changuinola I will maintain its future discharge rate at approximate 2015 levels to generate an average 1060GWh of energy across each year; this fact provided the basis for our alternative discharge management strategy (AES Changuinola, personal communication, February 22, 2017). We calculated the approximate discharge rate that would yield this energy output using the Hydropower Equation:

Equation 8

$$P_a = p*Q_{chan}*g*h*E$$

Where P_a is the actual power generated in watts (1060GWh across a year, divided by 8760 hours in a year), p is the density of water (1000kg/m^3), Q_{chan} is the mean monthly discharge rate at the dam (m^3/s), g is the acceleration of gravity (9.81m/s^2), h is the mean dam head (m), and E is the mean monthly dam efficiency. Head relates to the falling height of the water from the reservoir to the turbines. The maximum head at Changuinola I is 110m (Karlsson & Tallberg, 2011), and the head height change was reported in the data provided by AES Changuinola in 2015. The mean value across 2015 was used to estimate mean head in Equation 8. Monthly efficiency was calculated by estimating the theoretical power (P_{th}) that could be produced by each mean monthly discharge reported by AES Changuinola in 2015 (Equation 8, where E=1), and dividing the actual energy generated for that month by this amount (reported by AES Changuinola);

Equation 9

$$E = P_a/P_{th}$$

Which yields the dam efficiency (E) that can be used to estimate actual power production (P_a) for a given discharge rate (Q_{chan}), and vice versa. The mean efficiency across 2015, was used in Equation 8 to estimate the mean monthly discharge rate required to meet the energy generation target for Changuinola I (1060GWh annually).

Once this mean monthly discharge rate was calculated at Changuinola I, we inputted it into Equation 3 to estimate the mean monthly site discharge rate. We then used Equation 7 to estimate mean monthly site depth, whose residual change between monthly 2015 estimates were used to estimate depths across the study site. These depth values were integrated into our combined SDM to estimate mean monthly feeding abundance values in our alternative management strategy.

The Secretaría Nacional de Energía (SNE) in Panama predicts that energy demands will increase by 4.9% per year until 2050, but AES Changuinola reports that Changuinola I is currently operating at capacity (AES Changuinola, personal communication, February 22, 2017; SNE, 2016). Thus, alterations to the flow structure at Changuinola I were constrained by the natural discharge regime and the dam's target energy generation. Our alternative management strategy compares the estimated natural discharge rates across a year and the 2015 discharge regime to one where mean monthly Changuinola I discharge is constantly maintained at the mean discharge rate calculated in Equation 8. This represents a maximum reduction in discharge variance, and thus the maximum difference that could be observed in manatee feeding activity. Discharge variance is an important factor in manatee foraging activity, as habitat stability (or consistency of environment) and peaking flow management impacts species' survivorship and life history traits over the long term (Freeman et al., 2001). We considered the limits of the natural flow regime, Changuinola I operational capacity and the annual Changuinola I energy generation targets.

RESULTS

Species Distribution Model of Feeding

Significant variables and buffer radii differed between model subcomponents. Depth and slope were consistently significant (Table 1). Salinity was neither predictive in the PA nor FA models. Greater depth, turbidity, agriculture and urban development were all positively correlated with the presence and abundance of feeding marks, while increased width and forest cover were negatively correlated with manatee presence in both models. Salinity, slope, soil and non-forest vegetation showed opposite correlations between the PA and FA models (Table 1; for all Pearson correlation r values see Appendix, Table A5 and Table A6). Optimized buffer radii ranged from 121m to 2070m between approaches and classes (Table 1). Overall, we predicted feeding presence and absence moderately well, including only significant variables (r^2= 0.50, Table 1). Within cells where feeding occurred, we were also able to predict the quantity of feeding, albeit at a lower predictive power (r^2= 0.21, Table 1). The combined model, which yielded weighted feeding abundances, also had reasonable predictive power (r^2= 0.34). The study site, particularly the manmade channel system, is surrounded by intensive agricultural development. Our land use classification method was sensitive enough to identify the spectral signatures of thickly vegetated channel areas and highly turbid water ways as non-forest vegetation and soil classes, respectively (Figure 5).

Table 1 Summary of Pearson correlation values between the feeding marks used in each model and the environmental variables inputted into the GAM. An * indicates that the variable was significant in the GAM. Buffer radii are listed in brackets, and r-squared values (ordinary least squares) found in each of the GAMs with only significant variables run on *T. manatus* feeding.

Variable	PA Model	FA model
Water		
Depth	0.2139*	0.0511*
Salinity	-0.0808	0.0551
Turbidity	0.1381	0.1313*
Width	-0.1585*	-0.0560
Slope	0.0321*	-0.1933*
Land Use		
Soil	0.0213 (buffer: 464.5m)*	-0.1650 (buffer: 795.0m)
Forest	-0.0133 (buffer: 1737.3m)*	-0.3163 (buffer: 2069.9m)
Agriculture	0.0557 (buffer: 121.2m)*	0.3212 (buffer: 724.8m)
Non-forest	-0.2216 (buffer: 1462.4m)*	0.0670 (buffer: 1535.0m)
Urban	0.2502 (buffer: 1737.3m)*	0.2250 (buffer: 1416.3m)
R-squared	**0.5004**	**0.2050**

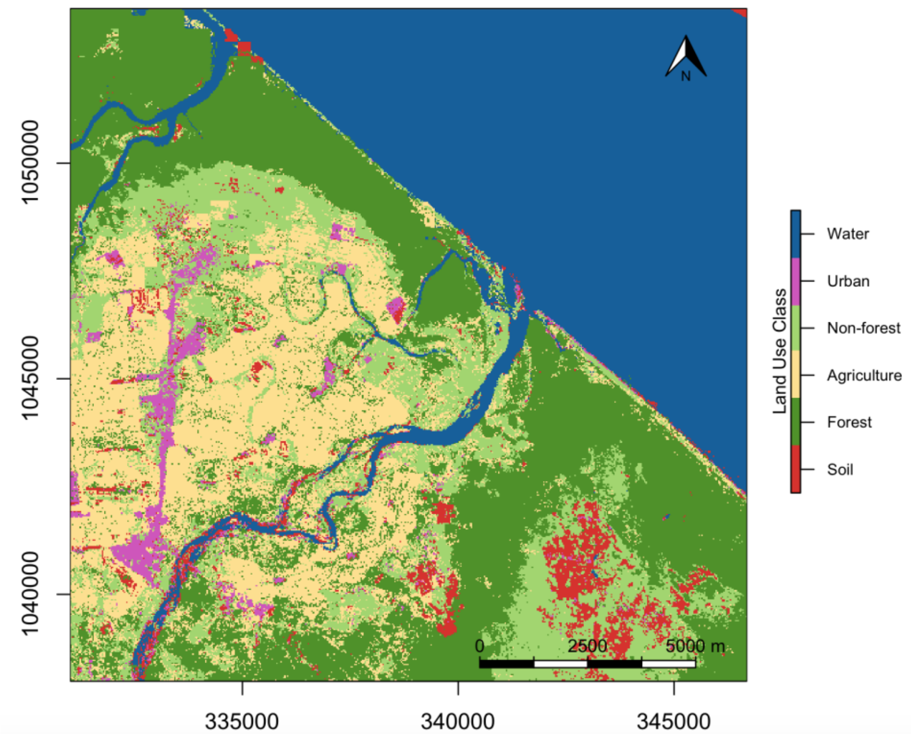

Figure 5 Land use classification of the *T. manatus* habitat in the Changuinola River, Panama in May 2015. Red= soil, dark green= forest, yellow= agriculture, light green= non-forest vegetation, purple= urban and blue= water.

While there was greater probability of feeding in the northwestern channels in the study site (PA model, Figure 6), feeding abundance predictions were uniform across the area in both the FA and combined models. There was a small cluster of greater feeding abundance predicted in the FA model, but when the probability of feeding occurrence was integrated (as in the combined model), this cluster became far less apparent (Figure 6).

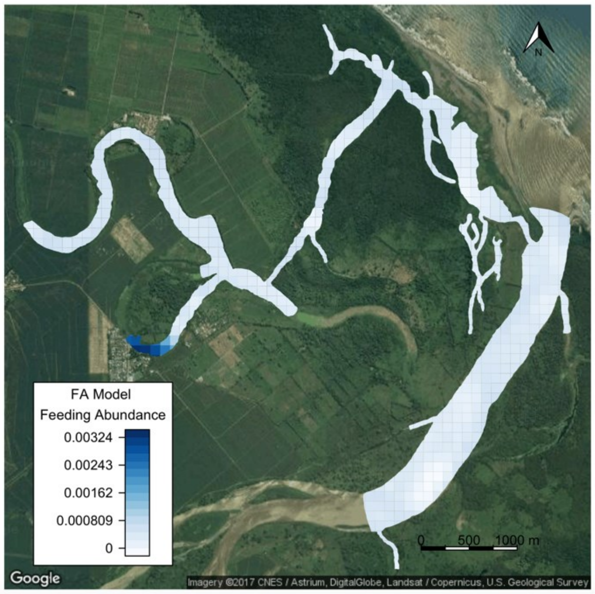

a

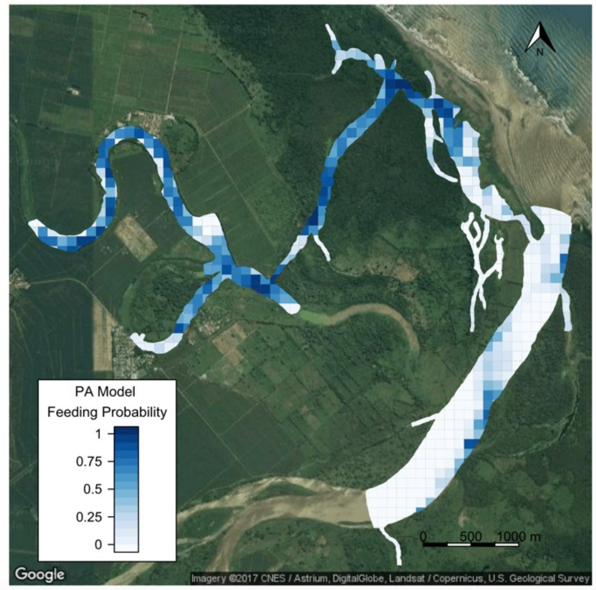

b

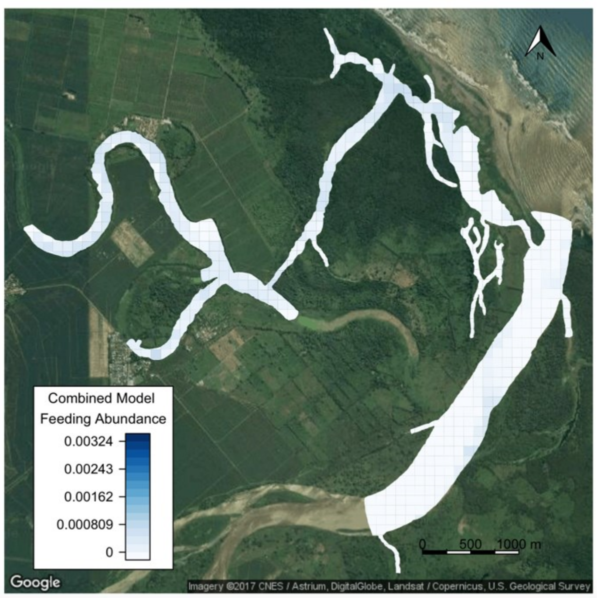

c

Figure 6 The GAM predictions for *T. manatus* feeding in the Changuinola River, Panama in May 2015; a) FA model, b) PA model, and c) combined model. Darker colours correspond to a greater amount of feeding abundance (marks/m^2) in the FA and combined models, and to a greater probability of feeding activity in the PA model.

Backcasting and alternative management

We used the flow accumulation grid to estimate discharge rates across the watershed (Figure 7) and the mean monthly flows at each gauge and the Changuinola I dam (Table A7), to confirm the linear regression relationship between flow accumulation and mean monthly discharge.

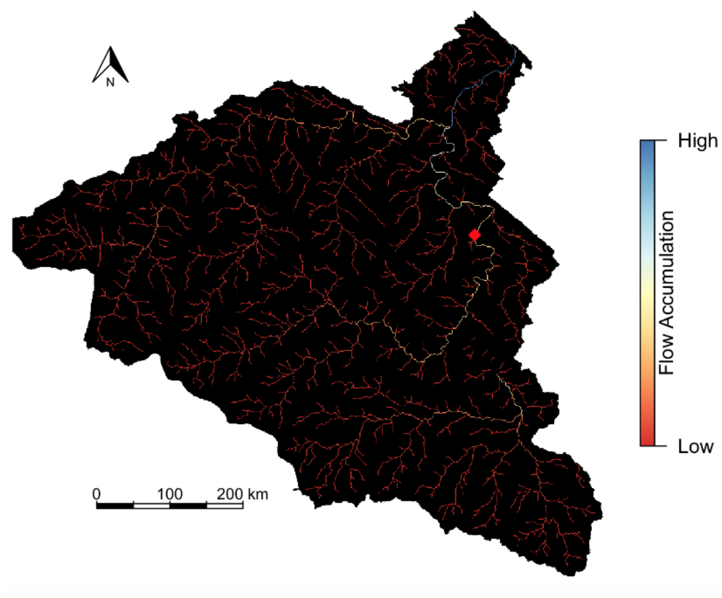

Figure 7 Flow accumulation grid in the Changuinola watershed, Panama generated from a sink-filled SRTM HYDROSHEDS 90m DEM (USGS, 2009). The red diamond represents the location of the Changuinola I dam.

The flow accumulation at each of the three stations 910102, 910401, and 910202 was 102 596 (52.1% flow), 17 326 (8.8% flow) and 28 454 cells (14.5% flow) respectively. The flow accumulation at the study site was 196 761 and at Changuinola I dam, it was 75 187. The value for p1 in Equations 2 and 3 was 0.326, representing about 24.6% of the total flow, and about one third of the flow accounted for by the ETESA stations. Gauge flow accumulation explained

97% of the variation in mean discharge for each month (Figure 8). Thus, flow accumulation could reasonably be used as a surrogate of mean monthly flow at each location in the watershed. The linear regression relationship is described by the following equation:

Equation 10

$$Q_{prop} = 1.014 * F_{prop} - 0.006$$

Where Q_{prop} is the mean monthly discharge at a given gauge (ETESA, n.d.), divided by the maximum monthly discharge across all gauges, and F_{prop} is the flow accumulation at a given gauge, divided by the maximum flow accumulation among the gauges (in this case, 102 596).

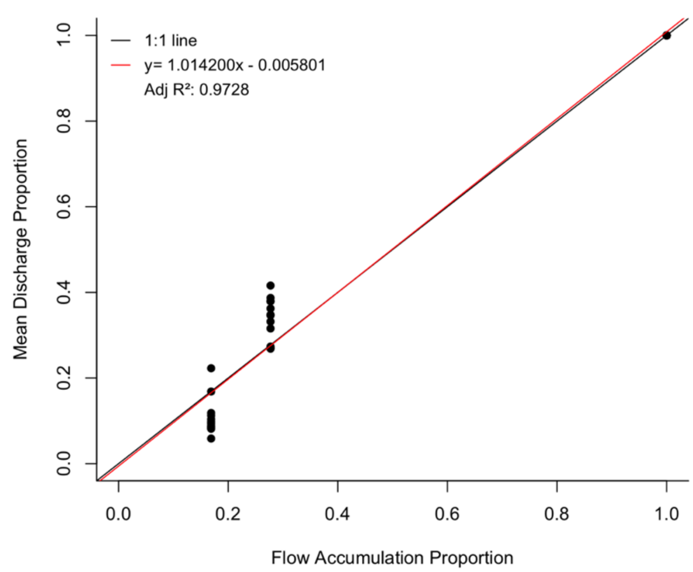

Figure 8 Proportional mean monthly discharge rate and flow accumulation at each of the three ETESA gauges in the Changuinola watershed across the length of their respective data collection periods (January 1st 2000-December 31st 2010 for stations 910102 and 910202, and June 12th 2001- November 11th 2002) prior to 2011 (ETESA, n.d.). Values were calculated using Equation 10. Linear regression between variables had a strong relationship (adjusted r^2= 0.9728).

Mean monthly flow at the Changuinola I dam was 132.41m^3/s, based on real time data provided by AES Changuinola (personal communication, Mar. 21, 2016). Using flow accumulation and Equation 10, we estimated what the expected mean monthly natural discharge at the Changuinola I dam location would have been prior to its operation. Across a given year, the mean natural flow predicted at that location was 142.54m^3/s. From September to December, our reported mean monthly flow at Changuinola I deviated more than one standard deviation (39.4m^3/s) below the expected mean natural flow for those given months. Mean reported November and December discharge rates were both greater than two standard deviations away from the predicted mean monthly natural flow for those months. Mean reported discharge rates for June and July were greater than one standard deviation above the mean monthly natural flow, with July being greater than three standard deviations above the mean natural flow for that month. Overall, the reported mean discharge rate with the dam present exhibited 2.52 times higher variance than would have been expected at Changuinola I if the dam were not present (Figure 9).

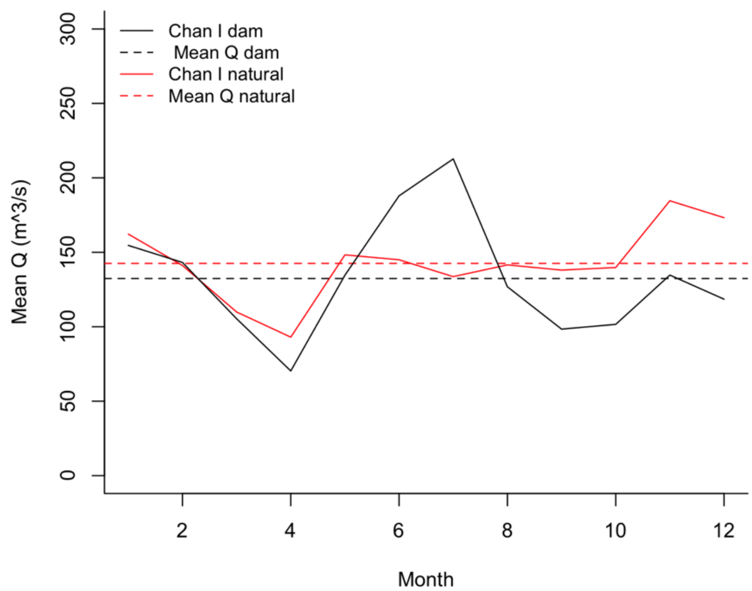

Figure 9 The mean monthly discharge rate (m^3/s) at the Changuinola I dam location, with the dam present in 2015 (Chan I dam and Mean Q dam; AES Changuinola, personal communication, Mar. 21, 2016) and predicted natural flows for 2015 (Chan I natural, and mean Q natural; calculated from Equations 2 and 3). Dotted lines indicate the mean discharge rate across the year for dam-modified ($132.41m^3/s \pm 39.4m^3/s$) and natural flows ($142.54m^3/s \pm 24.8m^3/s$).

Mean monthly study site discharge rates were estimated using Equations 2 and 3, for natural and dam-modified flows. We then calibrated the mean discharge rate at the study site for the month of May 2015 ($359.39m^3/s$; Equation 3), to the mean depth across the study site in our empirical measurements taken in May (1.43m), to estimate the coefficient K = 198.10 (Equation 7). Combining Equation 7 with the predicted site discharge rate (Table A8), we calculated the mean depth for each month in 2015, with and without the dam (Figure 10).

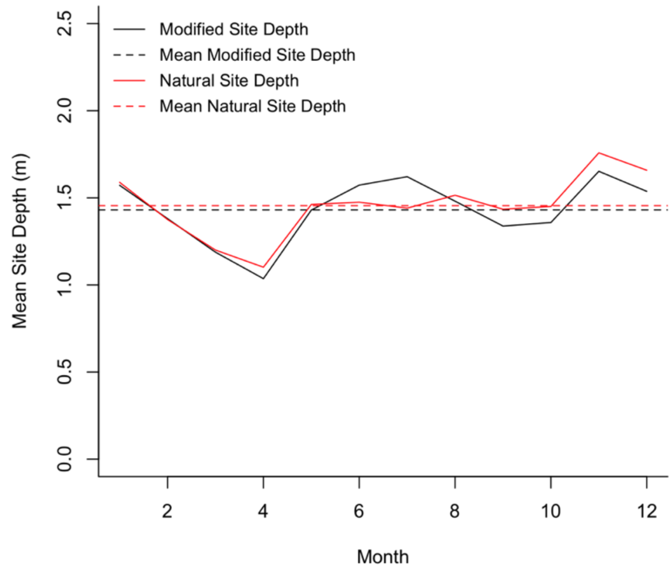

Figure 10 Mean monthly water depth (m) at study site with Changuinola I dam, Panama (modified; 1.43m) and without the dam (natural; 1.45m), calculated from Equation 7 and discharge estimates from Equations 2 and 3 for 2015 (AES Changuinola, personal communication, Mar. 21, 2016).

Despite the large difference in variance of flow at Changuinola I due to dam operations (Figure 10), this had only minor effect on depth at the site with manatees (variances of $0.034m^2$ and $0.032m^2$ for dam-modified and natural, respectively). Between June and August, the modified depths tended to be greater than would be expected with a natural flow rate; between September and December, this trend was reversed. We used these findings to model manatee foraging behaviour prior to the beginning of dam operation in November 2011, and given alternative management strategies.

Backcasting (2011)

We developed the backcasting scenario from two main inputs: land use classification in February 2011 (Figure 10) and predicted grid cell depths for February with natural flow at the dam site. In 2011, there was less agricultural, urban and soil land cover and more forest, non-forest vegetation and water land cover than in 2015. The biggest changes within a 5km radius of the study site (Figure 11) occurred in soil and forest, where soil increased by 1.3% and forest decreased by 1.1% over this 4-year period. In both years, the channels and lagoon were surrounded by less soil, non-forest vegetation, and forest cover, and more agriculture and urban land use than the lower Changuinola River main stem. In 2015, there was 3.4% and 1.4% more agriculture and urban land use; in 2011, there was 2.2% and 0.93% more agriculture and urban land use respectively surrounding the channels and lagoon than the main river stem. The 5km radius around the lower Changuinola River main stem saw an increase in forest cover of 0.5% over this 4-year period; whereas forest cover around the channels and lagoons decreased by 1.6%. The entire site exhibited an increase in soil land use classification between 2011 and 2015, however the soil increase around the main river (1.7%) was more than double that of the channels and lagoon (0.86%).

a)

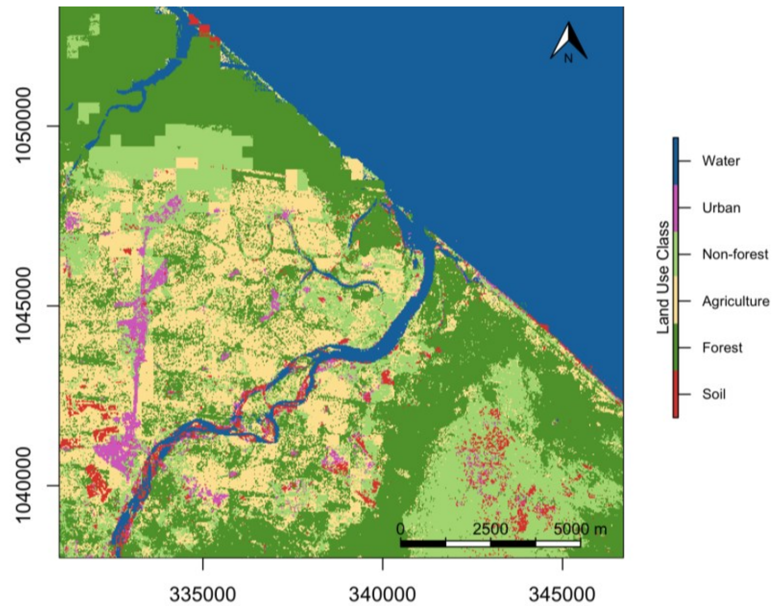

b)

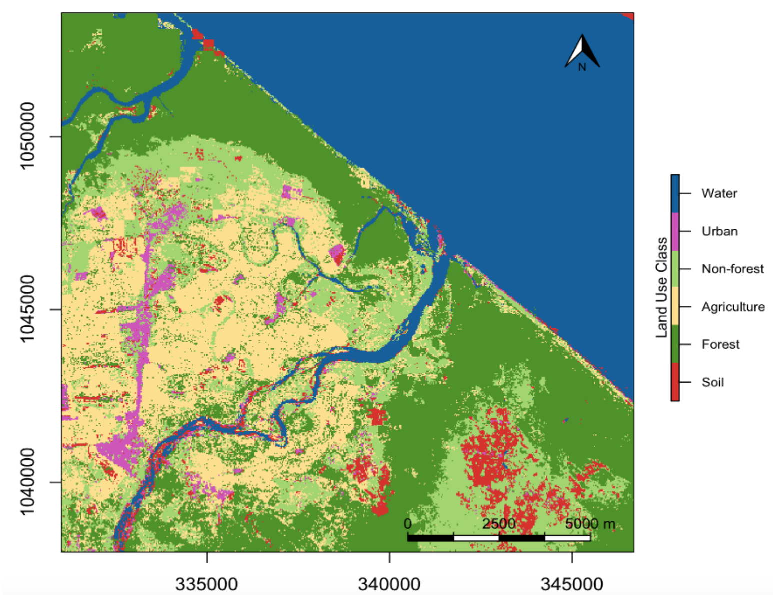

Figure 11 Land use classification of the *T. manatus* habitat in the lower Changuinola River, Panama in February 2011 (a) and May 2015 (b). Red= soil, dark green= forest, yellow= agriculture, light green= non-forest vegetation, purple= urban and blue= water.

We re-ran the SDMs built for 2015 with 2011 land use and local depth values (Figure 12). For the combined model, 2011 yielded both a larger mean (by a factor of 1.12 times) and maximum feeding abundance (by a factor of 4.0 times) than 2015; representing a 10.9% decrease in mean weighted feeding abundance and 75% decrease in max weighted feeding abundance over time. Thus, feeding intensity decreased between 2011 and 2015 according to our combined model. The small cluster of high feeding abundance identified in 2015 was also present in 2011 in the FA and combined models.

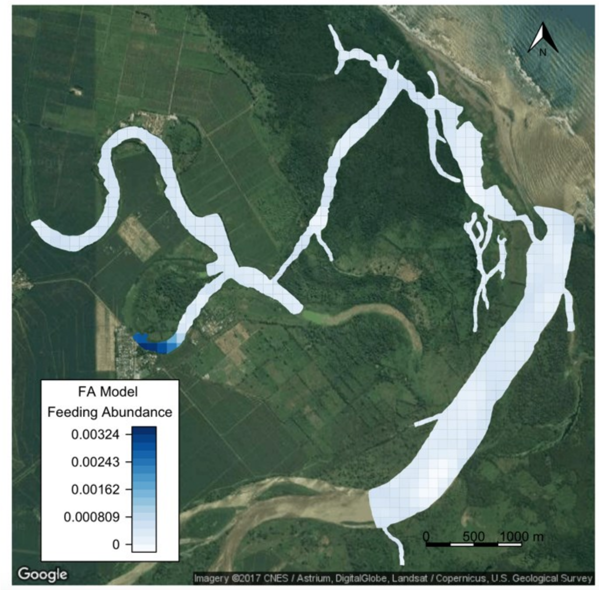

a

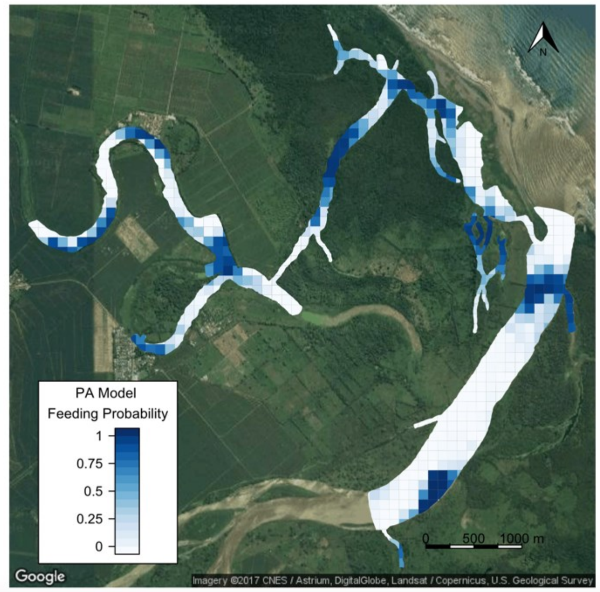

b

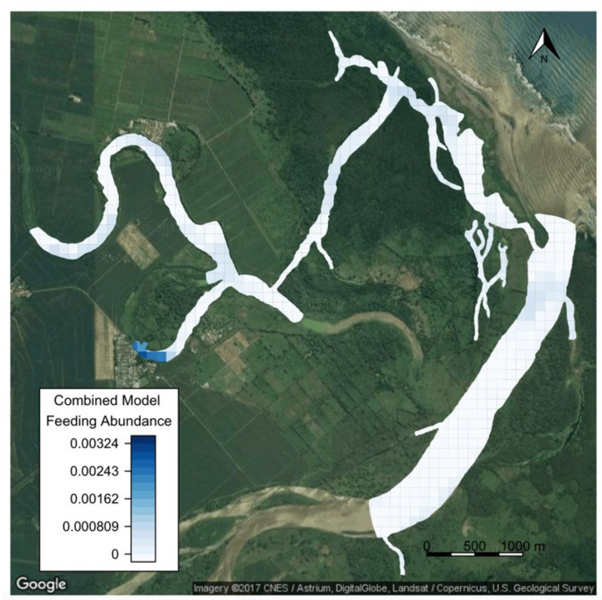

c

Figure 12 The GAM predictions for *T. manatus* feeding in the lower Changuinola River, Panama in February 2011; a) FA model, b) PA model, and c) combined model. Darker colours correspond to a greater amount of feeding abundance (marks/m^2) in the FA and combined models, and to a greater probability of feeding activity in the PA model.

Alternative management strategy

Power generation efficiency rates across 2015 ranged from 79.7% to 94.5%, and mean dam head height varied between 2.16m to 12.36m below the maximum height of 110m. The mean efficiency and dam head loss across the year was 90.5% and 6.91m, respectively. Panama produced a total of 1086.75MW in 2015, with AES Changuinola contributing about 11% (Autoridad Nacional de los Servicios Públicos, 2015). The mean monthly magnitude of energy produced at Changuinola I in 2015 was reported by AES Changuinola at approximately 122.51MW, and a mean discharge rate of 132.42m^3/s. As per discussions with AES Changuinola, the flow at Changuinola I would be maintained such that 1060GWh of energy are generated across the year, (AES Changuinola, personal communication, February 22, 2017) equivalent to about 121MW and 132.21m^3/s, based on the average head height (103.09m) and dam efficiency (90.5%) in 2015. With this in consideration, our alternative flow management scenario focused on minimizing the variance in the monthly dam discharge rate while meeting the target energy generation goals.

As previously shown in Figure 9, the dam-modified discharge rate at Changuinola I was far more variable than would be estimated naturally, with 2.52 times greater variance according to 2015 values. We compared the peaking flow management regime of 2015 with a maximally reduced variance structure where the mean monthly discharge at Changuinola I was maintained at 132.21m^3/s (the target discharge rate to yield 1060GWh annually). All monthly dam flows were set to the AES Changuinola reported discharge rate target (132.21m^3/s, corresponding to a site discharge rate of 362.59m^3/s), to represent maximum variance reduction (2.15 times less site flow variance). In this case, depth variance at the study site decreased by a factor of 2.28 times from 2015 variance, and feeding abundance variance decreased by a factor of 2.63 times from 2015 variance.

The estimated depth values for each month in our alternative management strategy, natural flow, and 2015 estimates were all inputted into our combined SDM model to yield monthly feeding abundances at the study site. With natural flows, mean weighted feeding abundances were 1.61% greater than that in 2015 and 1.18% greater than the alternative management strategy. With a maximum reduction of Changuinola I discharge variance, mean weighted feeding abundances were 0.42% greater than 2015 (Figure 13).

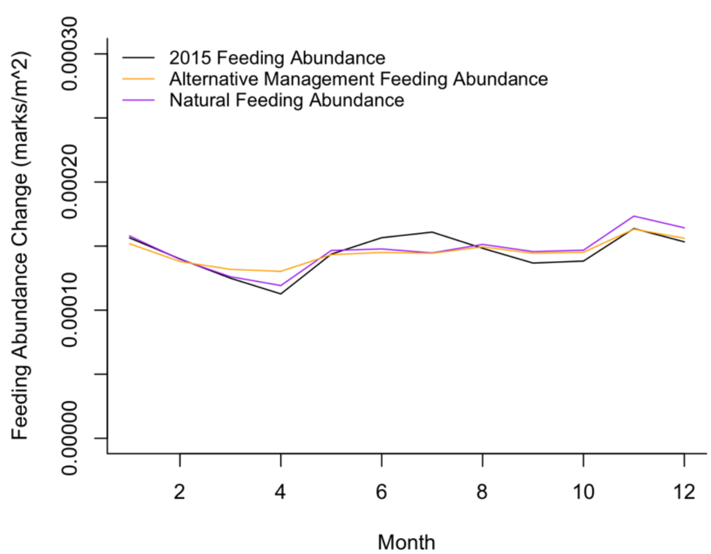

Figure 13 Estimated mean *T. manatus* foraging intensity (marks/m^2) at the lower Changuinola River study site, Panama in 2015 due to varying depth projections from Changuinola I dam flow management. Black indicates 2015 feeding abundances, yellow indicates alternative management feeding abundances (if Changuinola I discharge were maintained at 132.21m^3/s across the year), and purple indicates natural feeding abundances prior to Changuinola I dam operation.

DISCUSSION

Manatee distribution in the lower Changuinola River

This study yielded several important findings for manatees in the lower Changuinola River basin in Panama, with implications extending beyond this species and site. We developed an integrated GAM that predicts the weighted manatee feeding abundance, and accounts for data zero-inflation with a predictive power of $r^2 = 0.34$. The analyses demonstrated that the manatees are feeding across the lower Changuinola River, with only environmental variables predicting feeding abundance, and land use affecting the probability of feeding occurring, but not abundance. The land use in the lower Changuinola region, particularly in the channel and lagoon system is heavily influenced by agricultural development, which has increased even within the short period between 2011 and 2015. The backcasting scenario suggests that mean weighted feeding abundance decreased by 10.9% between 2011 and 2015. Our use of coarse resolution land use classes, BULC, and first order approximation of the river continuity relation and Manning's equation allowed the development of a basic, but functional, hydrological model that integrates fluvial geomorphology, hydropower flow management and species distribution modelling. Lastly, the maximum discharge variance modification that could be applied to the Changuinola I dam flow management scheme only has the potential to increase mean weighted manatee feeding abundance by approximately 0.42% but decrease feeding variance by 2.63 times.

Land use change and backcasting

Feeding abundance was primarily predicted based on water depth, turbidity and land slope. Depth and slope are closely linked to river discharge, suggesting that discharge is an important variable to monitor for manatee foraging habitat. Land use was not significantly predictive for feeding abundance, although the identification of turbidity as a significant predictive variable suggests an indirect effect due to local erosion and runoff. The lagoons and manmade channel system to the west of the Changuinola River main stem are particularly vulnerable to these processes, with 3.4% and 1.4% more agricultural and urban land use than the main river in 2015. The majority of the agricultural activity in the region consists of banana plantations, (Mou Sue et al., 1990) which have been subject to heavy applications of pesticides, fungicides and fertilizers for several decades (Cramer, 2013). These agrochemicals inevitably runoff into the local waterways and affect the local ecosystem, spurring accelerated aquatic vegetative growth. It is thus unsurprising that manatees are feeding in these highly polluted waterways, despite the threat of motorboat traffic and strikes on the Changuinola River and bordering channels (Reynolds III et al., 1995; Smethurst & Nietschmann, 1999; Guzmán & Rivera-Chavarria, 2014). Manatees in western Panama favour a foraging habitat centered within intense agricultural development, and downstream of direct wastewater effluent (Mou Sue et al., 1990; Collin et al., 2009; Cramer, 2013). While the water pollution may be aiding manatee foraging by accelerating vegetation growth, the ecological and physiological impacts of pollutant exposure have not been thoroughly studied and require immediate investigation for the conservation of the species and its habitat.

The economy in the lower Changuinola River is dominated by the banana industry (Cramer, 2013); however, this is not the only potential ecosystem service this region can provide. The local Bocas del Toro economy has boomed in the past decade with high flows of tourists, and specifically eco-tourists. Appropriate manatee habitat conservation and management could provide an opportunity for similar economic growth in the Changuinola community, and simultaneously support further scientific investigation. Florida manatees bring a net benefit of millions of dollars into the local economy each year, based mostly on eco-tourist attractions and establish a consistent source of funding for conservation and research activities (Solomon et al., 2004). The ecosystem service provided by these endangered mammals in the United States could be extrapolated to Bocas del Toro, building on the eco-tourism industry that is already present in the province.

Model performance and new applications

Despite some methodological shortcomings, the models developed herein were successfully predictive and comparable to the feeding occurrences and abundances observed in the field survey. The land use analysis techniques applied were modified to accommodate for the natural limitations of remote sensing in tropical ecosystems. While the land use classes selected were coarse and did not encompass different stages of forest succession or classification, they were predictive and essential to model building, suggesting that broad land cover classifications can still be useful in model development and conservation planning (Sliva & Williams, 2001; Hopkins II, 2009). In cases where land cover data is limited, or missing altogether, a basic land use map can provide valuable insight into a species' distribution in a system. To build on these results, classifications could be added to the analysis using finer resolution optical imagery, land use classes or radar technology. The integration of radar data would be particularly interesting, as this is not subject to cloud cover limitations. In cases where cloud cover is a significant limitation to data acquisition, the BULC method proved to be a highly effective tool to fill in missing data components. This technique has only recently been developed, and has great promise for future research and management programs.

Fluvial geomorphological concepts are frequently applied in SDMs for fish species, but this is much less often the case for aquatic mammals (Oberdorff et al., 2001; Buisson et al., 2008; Bond et al., 2011). One exception is the recent Charbonnel et al. (2016) study that integrated species distribution modelling, hydrology, and land cover to generate predictions for a semi-aquatic endemic mammalian species in the French Pyrenees. Both the Charbonnel et al. (2016) study and our study demonstrate the value of integrating diverse predictive tools in cases of conservation management. Building on the Charbonnel et al. (2016) methodology, we took our analysis one step further to predict future management strategies for local disturbance activities (in this case, hydroelectric power generation), and performed our own land use classification at a greater spatial resolution. Even though discharge, precipitation, temperature and evapotranspiration data in the region were either incomplete or missing altogether, we could reasonably estimate natural discharge at Changuinola I based on the similarity between our mean natural flow (142.54m^3/s) and the upper bound of mean dam discharge cited by AES Changuinola (132.21m^3/s). While this model could be improved by the integration of soils and climatic data, such as in a Soil and Water Assessment Tool (SWAT) (Charbonnel et al., 2016), our generalized approach allows the integration of fluvial hydrology into SDMs in cases where data at fine resolution may be missing.

Future management

With an annual mean discharge across 2015 at 132.41m^3/s, and a stated limitation of the Changuinola I dam at an average energy production of 1060GWh, there can be no further electricity output at this hydropower plant. Unfortunately, energy demand in Panama is projected to increase by an average of 4.9% per year until 2050 (SNE, 2016), which has already been exceeded between 2014 and 2015 (9.18%) and 2015 and 2016 (5.48%) (BNAM, 2017). Since a future scenario of flow modification could not be generated for our study system, all that can be done is alteration of the current discharge scheme. It was found that a maximum reduction in discharge variance at the Changuinola I dam could only increase the estimated mean weighted feeding abundance by 0.42% (2.63 times less foraging variance than 2015), and represents a median value between current Changuinola I modified flows and estimated natural flow rates. Natural discharge rates produced the greatest mean weighted feeding abundance, 1.61% greater than 2015 levels. Hydropower flow modification did not have a significant detrimental impact on absolute mean weighted feeding abundance in this case study, but modifications to discharge management could improve habitat stability across a given year. This finding is supported by the principle of Jensen's Inequality, where an environmental variable's variance has a greater effect than its average alone on species' behaviour (Ruel & Ayres, 1999). Thus, habitat stability is at risk from hydropower impoundment, particularly dams operating under a peak load management scheme (Freeman et al., 2001). Reducing foraging habitat variance in our future management scenario promotes habitat persistence while also maintaining the ecosystem service of river flow for energy production. It reflects a realistic and attainable management strategy for the study system.

Caveats of research

While the measures of fit attained in this analysis are encouraging, there are several caveats that should be addressed. First, the age of the feeding marks was not determined, thus some areas may have been former feeding grounds. That being said, manatees are known to return to the same feeding areas, so this may have provided a more complete picture of their preferred feeding grounds. Secondly, feeding marks were only recorded on floating, not subaquatic, vegetation where the motorboat could navigate during the survey (we were prohibited from certain narrow channels which were so thickly vegetated, we could not travel further). This presents bias in the survey, as it is unknown where the manatees are feeding underwater, and their foraging behaviour in the densely vegetated channels could not be recorded. This could not be helped, given river turbidity and navigability, but could be a potential opportunity for further investigation into seagrass mapping and infrared drone detection of manatees underwater (Lefebvre et al., 1999; Koski et al., 2009). Cross-validation of the model was not integrated into the analyses, because there was not enough data available to allow for an accurate examination of model performance across such a small study site. Repetition of the field surveys conducted, and the application of drone technology to estimate manatee abundances and distribution in the turbid waters of the lower Changuinola would both be highly recommended developments in the future, as time and resource restrictions did not allow multiple surveys.

Another potential cause for concern may be the land use classes selected and the use of varying buffer sizes for each class. We would argue that this constitutes a strength of our analysis, as the coarse land use classes were consciously selected to increase efficiency of classification, and facilitate easier methodology extrapolation to other studies. Additionally, these land use classes are commonly used to analyse species' distributions and river water quality (Sliva & Williams, 2001; Hopkins II, 2009). Further, there are issues with limiting land use analysis and riparian buffers to a simple 100m model (Sliva & Williams, 2001). Often, this 100m buffer is not enough to capture the effects of local watershed land use on river quality, and the catchment level is more appropriate (Hunsaker & Levine, 1995). The opposite has also been found, where riparian buffers performed equally as well, or better, than the watershed level analysis (Johnson et al., 1997), thus fuelling a "buffer versus catchment" debate in scholarly literature (Sliva & Williams, 2001). As such, our approach to address this issue was to optimize buffer selection for each land use class using the optim function in R. While this may be open to the critique of over-fitting, it represented a median approach between riparian buffer versus catchment analysis.

The overlaying and filling of land use images is often a task only for remote sensing specialists, but the BULC algorithm developed by Cardille and Fortin (2016) allowed basic land use classification maps, and data sparse regions of analysis (e.g. intense cloud, haze cover or missing data lines from Landsat 7 imagery) to be compiled into a continuously updating image with only the most probable and recent land use classes incorporated. The BULC algorithm provided a means of circumventing what would have otherwise been an extremely time and computationally expensive process to potentially yield one full classified image (Cardille & Fortin, 2016).

Lastly, to build flow modification and hydrology into our model, several assumptions were made. The first was that all depths across the site varied by the residuals about the mean water depth in the lower Changuinola River. This assumption also implied that water levels in the main stem and in the channels and lagoon system varied by the same amount. This may not represent reality, but given the artificial and ungauged nature of the channels and main stem, this was the best possible approach for approximation. Furthermore, with no discharge gauges existing in the study site, no validation step could be applied to the model. However, ungauged river catchments are not an uncommon issue in hydrological research, and the integration of a flow accumulation grid to interpolate discharge rates in ungauged channels has been applied in systems ranging from the Himalayas (Das & Paul, 2006), Germany (Kuemmerlen et al., 2014) and China (Schmalz et al., 2015). The next step for our research would be to install discharge gauges in the lower Changuinola River as validation for our approach, and to build on the current SDM with the integration of soil and precipitation analyses into the hydrological model. SWAT could accomplish this integration, and has been successfully applied in SDMs in other data-restricted areas (Schmalz et al., 2015; Charbonnel et al., 2016). Thus, despite these shortcomings, the findings from this study lead to several interesting future avenues for conservation research, in Panama and beyond.

Implications for conservation in tropical countries

The concerns regarding conservation of Antillean manatees in this case study mirror the common struggles encountered by many tropical conservation biologists. Large scale flow manipulation and land use change are significant ecological drivers for habitat and species conservation. The pollution and deforestation resulting from massive agricultural monoculture plantations could have devastating biodiversity consequences (Lenzen et al., 2012), and damage the potential for an economically and scientifically valuable eco-tourism industry.

Long term data acquisition and analysis is relatively rare in the tropics; this study demonstrates understanding the current state of affairs can unveil targeted local and attainable conservation efforts. The application of SDMs, remote sensing technology, foraging habitat proxies and fluvial geomorphology to analyse hydropower operations and management illustrate the ecological and hydrological conditions of an ecosystem and species. The unique toolset employed addresses the common challenges facing many conservation biologists today, and sets the stage for future research and economic endeavours.

CONCLUDING REMARKS

In this thesis, we examined the foraging distribution of Antillean manatees in the lower Changuinola River, Panama, and the changes of that distribution across time with land use and river discharge modification. Our models indicated that mean weighted manatee feeding abundance decreased by 10.9% between February 2011 (before dam operation) and May 2015 (after dam operation). SDMs built for 2015 suggested that only water depth, turbidity and land slope were predictive for feeding abundance, while land use was also predictive of manatee foraging presence. The final GAM produced accounted for significant zero-inflation in the data and yielded a predictive power of r^2=0.34.

Implications of flow modification from hydropower generation in the watershed indicate that the Changuinola I dam peaking flow management practice causes 2.52 times the variance in flow than would be expected naturally at the dam location, and maximum reduction of this variance caused a decrease in mean weighted feeding abundance variance at the study site by 2.63 times the variance in 2015, and a 0.42% increase in weighted feeding abundance from 2015. Our findings indicate that flow management at the Changuinola I dam would have a marginal effect on absolute mean weighted feeding abundances, but a significant effect on foraging habitat stability. Our study suggests that preserving manatees in western Panama has the potential to provide a new eco-tourism ecosystem service, while maintaining the current hydropower production service that is already realised.

WORKS CITED

AES Changuinola. (2013). *Central Hidroeléctrica Changuinola I.* Retrieved from http://www.aeschanguinola.com/changuinola-i.html

Albon, S. D., Brewer, M. J., O'Brien, S., Nolan, a. J., & Cope, D. (2007). Quantifying the grazing impacts associated with different herbivores on rangelands. *Journal of Applied Ecology, 44*(6), 1176–1187. DOI: 10.1111/j.1365-2664.2007.01318.x

Ansar, A., Flyvbjerg, B., Budzier, A., & Lunn, D. (2014). Should we build more large dams? The actual costs of hydropower megaproject development. *Energy Policy, 69*, 43–56. DOI: 10.1016/j.enpol.2013.10.069

Aswani, S., Christie, P., Muthiga, N. a., Mahon, R., Primavera, J. H., Cramer, L. a., … Hacker, S. (2012). The way forward with ecosystem-based management in tropical contexts: Reconciling with existing management systems. *Marine Policy, 36*(1), 1–10. DOI: 10.1016/j.marpol.2011.02.014

Barry, S. C., & Welsh, A. H. (2002). Generalized additive modelling and zero inflated count data. *Ecological Modelling*, *157*(2), 179–188. DOI: 10.1016/S0304-3800(02)00194-1

BNAM. (2017). *Electric Power Data.* Retrieved on February 22, 2017 from https://subscriber.bnamericas.com/Subscriber/en/data/electricpower/

Bond, N., Thomson, J., Reich, P., & Stein, J. (2011). Using species distribution models to infer potential climate change-induced range shifts of freshwater fish in south-eastern Australia. *Marine and Freshwater Research*, *62*(9), 1043–1061. DOI: 10.1071/MF10286

Bowker, D. E., Davis, R. E., Myrick, D. L., Stacy, K., & Jones, W. T. (1985). *Spectral reflectances of natural targets for use in remote sensing studies* (Technical Report NASA-RP-1139, L-15920, NAS 1.61:1139). NASA Langley Research Center, Hampton, VA. 185p. Retrieved from http://ntrs.nasa.gov/search.jsp?R=19850022138

Brooks, T. M., Mittermeier, R. A., Mittermeier, C. G., da Fonseca, G. A. B., Rylands, A. B., Konstant, W. R., … Hilton-Taylor, C. (2002). Habitat Loss and Extinction in the Hotspots of Biodiversity. *Conservation Biology*, *16*(4), 909–923. DOI: 10.1046/j.1523-1739.2002.00530.x

Buisson, L., Blanc, L., & Grenouillet, G. (2008). Modelling stream fish species distribution in a river network: the relative effects of temperature versus physical factors. *Ecology of Freshwater Fish*, *17*(2), 244–257. DOI: 10.1111/j.1600-0633.2007.00276.x

Cardille, J. A., & Fortin, J. A. (2016). Bayesian updating of land-cover estimates in a data-rich environment. *Remote Sensing of Environment*, *186*, 234–249. DOI: 10.1016/j.rse.2016.08.021

Castelblanco-Martínez, D. N., Nourisson, C., Quintana-Rizzo, E., Padilla-Saldivar, J., & Schmitter-Soto, J. J. (2012). Potential effects of human pressure and habitat fragmentation on population viability of the Antillean manatee *Trichechus manatus manatus*: a predictive model. *Endangered Species Research*, *18*(2), 129-145.

Castelblanco-Martínez, D. N., dos Reis, V., & de Thoisy, B. (2017). How to detect an elusive aquatic mammal in complex environments? A study of the Endangered Antillean manatee *Trichechus manatus manatus* in French Guiana. *Oryx*, 1–11. DOI: 10.1017/S0030605316000922

Charbonnel, A., Laffaille, P., Biffi, M., Blanc, F., Maire, A., Némoz, M., … Buisson, L. (2016). Can Recent Global Changes Explain the Dramatic Range Contraction of an Endangered Semi-Aquatic Mammal Species in the French Pyrenees? *PLOS ONE*, *11*(7), e0159941. DOI: 10.1371/journal.pone.0159941

Christie, P., Fluharty, D. L., White, A. T., Eisma-Osorio, L., & Jatulan, W. (2007). Assessing the feasibility of ecosystem-based fisheries management in tropical contexts. *Marine Policy, 31*(3), 239–250. DOI: 10.1016/j.marpol.2006.08.001

Collin, R. (2005). Ecological Monitoring and Biodiversity Surveys at the Smithsonian Tropical Research Institute's Bocas del Toro Research Station. *Caribbean Journal of Science*, *41*(3), 367–373.

Collin, R., Croz, L. D., Gondola, P., & Rosario, J. B. Del. (2009). Climate and Hydrological Factors Affecting Variation in Chlorophyll Concentration and Water Clarity in the Bahia Almirante, Panama. *Smithsonian Contributions to the Marine Sciences*, *38*, 323–334.

Costanza, R., & Daly, H. (2003). Natural capital and sustainable development. *Conservation Biology, 6*(1), 37–46. DOI: 10.1046/j.1523-1739.1992.610037.x

Cramer, K. L. (2013). History of human occupation and environmental change in western and central Caribbean Panama. *Bulletin of Marine Science, 89*(4), 955–982. DOI: 10.5343/bms.2012.1028

Das, S., & Paul, P. K. (2006). Selection of Site for Small Hydel Using GIS in the Himalayan Region of India. *Journal of Spatial Hydrology*, *6*(1), 18–28.

D'Croz, L., Del Rosario, J. B., & Góndola, P. (2005). The effect of fresh water runoff on the distribution of dissolved inorganic nutrients and plankton in the Bocas del Toro Archipielago, Caribbean Panama. *Caribbean Journal of Science*, *41*(3), 414–429.

de Groot, R. S., Alkemade, R., Braat, L., Hein, L., & Willemen, L. (2010). Challenges in integrating the concept of ecosystem services and values in landscape planning, management and decision making. *Ecological Complexity*, *7*(3), 260–272. DOI: 10.1016/j.ecocom.2009.10.006

Deutsch, C.J., Self-Sullivan, C. & Mignucci-Giannoni, A. 2008. *Trichechus manatus*. In: *IUCN 2013. IUCN Red List of Threatened Species. Version 2013.2*. Retrieved from http://www.iucnredlist.org/details/22103/0

Díaz-Ferguson, E., Hunter, M., & Guzmán, H. (in press). Genetic composition and connectivity of the Antillean manatee (*Trichechus manatus manatus*) in Panama. *Aquatic Mammals.*

Dudgeon, D. (2000). Large-Scale Hydrological Changes in Tropical Asia: Prospects for Riverine Biodiversity. *BioScience*, *50*(9), 793-806.

Dudgeon, D., Arthington, A. H., Gessner, M. O., Kawabata, Z.-I., Knowler, D. J., Lévêque, C., … Sullivan, C. A. (2006). Freshwater biodiversity: importance, threats, status and conservation challenges. *Biological Reviews*, *81*(2), 163. DOI: 10.1017/S1464793105006950

Egoh, B., Reyers, B., Rouget, M., Bode, M., & Richardson, D. M. (2009). Spatial congruence between biodiversity and ecosystem services in South Africa. *Biological Conservation*, *142*(3), 553–562. DOI: 10.1016/j.biocon.2008.11.009

ESA. (2010). *GlobCover*. Retrieved from http://due.esrin.esa.int/page_globcover.php

ESRI. (2016). *Creating a depressionless DEM*. Retrieved from http://pro.arcgis.com/en/pro-app/tool-reference/spatial-analyst/creating-a-depressionless-dem.htm

ETESA. (n.d.). *Open Data.* Retrieved from https://www.hidromet.com.pa/open_data.php

ETESA. (2008). *Resumen Técnico Análisis Regional de Crecidas Máximas de Panamá Periodo 1971-2006* (report). Retrieved from http://www.hidromet.com.pa/documentos/Analisis_Crecidas_Maximas_Panama.pdf

ETESA. (2009). *Cuencas Hidrográficas de Panamá.* Retrieved from http://www.hidromet.com.pa/cuencas.php

Freeman, M. C., Bowen, Z. H., Bovee, K. D., & Irwin, E. R. (2001). Flow and habitat effects on juvenile fish abundance in natural and altered flow regimes. *Ecological Applications*, *11*(1), 179–190. DOI: 10.2307/3061065

Gómez-Baggethun, E., de Groot, R., Lomas, P. L., & Montes, C. (2010). The history of ecosystem services in economic theory and practice: From early notions to markets and payment schemes. *Ecological Economics, 69*(6), 1209–1218. DOI: 10.1016/j.ecolecon.2009.11.007

Gonzalez-Socoloske, D., Olivera-Gómez, L. D., Reid, J. P., Espinoza-Marin, C., Ruiz, K. E., & Glander, K. E. (2015). First successful capture and satellite tracking of a West Indian manatee (Trichechus manatus) in Panama: feasibility of capture and telemetry techniques. *Latin American Journal of Aquatic Mammals, 10*(1), 52–57.

Guzmán, H. M., Barnes, P. A. G., Lovelock, C. E., & Feller, I. C. (2005). A Site Description of the CARICOMP Mangrove, Seagrass and Coral Reef Sites in Bocas del Toro, Panama. *Caribbean Journal of Science*, *41*(3), 430–440.

Guzmán, H. M., & Jiménez, C. E. (1992). Contamination of coral reefs by heavy metals along the Caribbean coast of Central America (Costa Rica and Panama). *Marine Pollution Bulletin*, *24*(11), 554–561. DOI: 10.1016/0025-326X(92)90708-E

Guzmán, H.M., & Rivera-Chavarría, M. (2014). *Sistema Integrado de Monitoreo del Manatí (Trichechus manatus) en el Area de Influencia de la Cuenca del Río Sixaola (Costa Rica y Panama)* (No. FN-SIXAOLA-STRI-002-2013). Proyecto Manejo Integrado de Ecosistemas en la Cuenca Binacional del Río Sixaola.

Guzmán, H., & Condit, R. (in press). Abundance of manatees (*Trichechus manatus*) in Panama estimated from side-scan sonar. *Wildlife Society Bulletin*.

Harris Geospatial Solutions. (2016). *Example: Multispectral Sensors and FLAASH*. Retrieved from http://www.harrisgeospatial.com/docs/ExampleMSSensorsFLAASH.html

Hartman, D. S. (1979). *Ecology and Behaviour of the Manatee (Trichechus manatus) in Florida* (Special Publication 5). Pittsburgh, PA: American Society of Mammalogists. DOI: 10.5962/bhl.title.39474

He, K. S., Bradley, B. A., Cord, A. F., Rocchini, D., Tuanmu, M.-N., Schmidtlein, S., … Pettorelli, N. (2015). Will remote sensing shape the next generation of species distribution models? *Remote Sensing in Ecology and Conservation, 1*(1), 4–18. DOI: 10.1002/rse2.7

Hickin, Edward, J. (1995). Hydrology and the size of a river. In *River geomorphology* (pp. 18–43). Chichester: John Wiley & Sons Ltd. Retrieved from http://www.sfu.ca/~hickin/RIVERS/Rivers2%28Hydrology%29.pdf

Hines, J. E., Nichols, J. D., Royle, J. A., MacKenzie, D. I., Gopalaswamy, A. M., Kumar, N. S., & Karanth, K. U. (2010). Tigers on trails: occupancy modeling for cluster sampling. *Ecological Applications, 20*(5), 1456–1466. DOI: 10.1890/09-0321.1

Hunter, M. E., Auil-Gomez, N. E., Tucker, K. P., Bonde, R. K., Powell, J., & McGuire, P. M. (2010). Low genetic variation and evidence of limited dispersal in the regionally important Belize manatee. *Animal Conservation, 13*(6), 592-602.

Hunsaker, C. T., & Levine, D. A. (1995). Hierarchical Approaches to the Study of Water Quality in Rivers. *BioScience*, *45*(3), 193–203. DOI: 10.2307/1312558

IUCN Species Survival Commission. (2000). *IUCN Red List Categories and Criteria* (Version 3.1). Retrieved from http://jr.iucnredlist.org/documents/redlist_cats_crit_en.pdf

IUCN Red List of Threatened Species. (2016). *The IUCN Red List of Threatened Species*. Retrieved from http://www.iucnredlist.org/

Jiménez, I. (2005). Development of predictive models to explain the distribution of the West Indian manatee *Trichechus manatus* in tropical watercourses. *Biological Conservation, 125*(4), 491–503. DOI: 10.1016/j.biocon.2005.04.012

Johnson, L. B., Richards, C., Host, G. E., & Arthur, J. W. (1997). Landscape influences on water chemistry in Midwestern stream ecosystems. *Freshwater Biology*, *37*(1), 193–208. DOI: 10.1046/j.1365-2427.1997.d01-539.x

Julien, P. Y. (2002). *River mechanics* (1st ed.). Cambridge, UK: Cambridge University Press.

Karanth, K. U., Gopalaswamy, A. M., Kumar, N. S., Vaidyanathan, S., Nichols, J. D., & Mackenzie, D. I. (2011). Monitoring carnivore populations at the landscape scale: Occupancy modelling of tigers from sign surveys. *Journal of Applied Ecology, 48*(4), 1048–1056. DOI: 10.1111/j.1365-2664.2011.02002.x

Karlsson, T., & Tallberg, J. (2011). Concrete Face Rock-fill dam compared to Roller Compacted Concrete dam (Master's Dissertation). Retrieved from http://publications.lib.chalmers.se/records/fulltext/146361.pdf (Master's Thesis 2011:120).

Kaufmann, K. W., & Thompson, R. C. (2005). Water Temperature Variation and the Meteorological and Hydrographic Environment of Bocas del Toro, Panama. *Caribbean Journal of Science*, *41*(3), 392-413.

Kerr, J. T., & Ostrovsky, M. (2003). From space to species: ecological applications for remote sensing. *Trends in Ecology & Evolution, 18*(6), 299–305. DOI: 10.1016/S0169-5347(03)00071-5

Koski, W. R., Allen, T., Ireland, D., Buck, G., Smith, P. R., Macrander, M.,… McDonald, T. L. (2009). Evaluation of an Unmanned Airborne System for Monitoring Marine Mammals. *Aquatic Mammals, 35*(3), 347-357. DOI: 10.1578/AM.35.3.2009.347

Kuemmerlen, M., Schmalz, B., Guse, B., Cai, Q., Fohrer, N., & Jähnig, S. C. (2014). Integrating catchment properties in small scale species distribution models of stream macroinvertebrates. *Ecological Modelling*, *277*, 77–86. DOI: 10.1016/j.ecolmodel.2014.01.020

LaCommare, K. S., Self-Sullivan, C., & Brault, S. (2008). Distribution and habitat use of Antillean manatees (*Trichechus manatus manatus*) in the Drowned Cayes area of Belize, Central America. *Aquatic Mammals, 34*(1), 35.

Lefebvre, Lynn, W., Reid, James, P., Kenworthy, W. J., & Powell, James, A. (1999). Characterizing Manatee habitat use and seagrass grazing in Florida and Puerto Rico: implications for conservation and management. *Pacific Conservation Biology, 5*(4), 289–298. DOI: 10.1071/PC000289

Lenzen, M., Moran, D., Kanemoto, K., Foran, B., Lobefaro, L., & Geschke, A. (2012). International trade drives biodiversity threats in developing nations. *Nature, 486*(7401), 109–112. DOI: 10.1038/nature11145

Leopold, Luna, B., & Maddock, Thomas, J. (1953). *The Hydraulic Geometry of Stream Channels and Some Physiographic Implications (Paper 252)*. Washington: United States Geological Survey. 56p.

Malmqvist, B., & Rundle, S. (2002). Threats to the running water ecosystems of the world. *Environmental Conservation*, *29*(2), 134–153. DOI: 10.1017/S0376892902000097

Marchese, C. (2015). Biodiversity hotspots: A shortcut for a more complicated concept. *Global Ecology and Conservation*, *3*, 297–309. DOI: 10.1016/j.gecco.2014.12.008

Marsh, H., O'Shea, T. J., & Best, R. C. (1986). Research on sirenians. *Ambio*, *15*(3), 177-180.

McLeod, K., Lubchenco, J., Palumbi, S., & Rosenberg, A. (2005). Scientific Consensus Statement on Marine Ecosystem-Based Management. *Compass*, 1–21. DOI: 10.1080/13880290109353975

Mittermeier, R. A., Myers, N., Thomsen, J. B., da Fonseca, G. A. B., & Olivieri, S. (1998). Biodiversity Hotspots and Major Tropical Wilderness Areas: Approaches to Setting Conservation Priorities. *Conservation Biology, 12*(3), 516–520. DOI: 10.1046/j.1523-1739.1998.012003516.x

Mittermeier, Russell, A., Gil, P. R., Hoffman, M., Pilgrim, J., Brooks, T., Mittermeier, Cristina, G., … da Fonseca, Gustavo, A. B. (2004). *Hotspots Revisited: Earth's Biologically Richest and Most Endangered Terrestrial Ecoregions*. Mexico City: CEMEX. Retrieved from https://www.researchgate.net/publication/275651117_Hotspots_Revisited_Earth%27s_Biologically_Richest_and_Most_Endangered_Terrestrial_Ecoregions

Moritz, S., Sardá, A., Bartz-Beielstein, T., Zaefferer, M., & Stork, J. (2015). Comparison of different Methods for Univariate Time Series Imputation in R. *Cologne University of Applied Sciences*, 1–20. Retrieved from www.th-koeln.de. arXiv preprint arXiv:1510.03924

Mou Sue, L., Chen, D. H., Bonde, R. K., & O'Shea, T. J. (1990). Distribution and status of manatees (Trichechus manatus) in Panama. *Marine Mammal Science*, *6*(3), 234-241.

Myers, N., Mittermeier, R. A., Mittermeier, C. G., Da Fonseca, G. A. B., & Kent, J. (2000). Biodiversity hotspots for conservation priorities. *Nature, 403*(24), 853–858.

Nelson, E., Mendoza, G., Regetz, J., Polasky, S., Tallis, H., Cameron, Dr., … Shaw, Mr. (2009). Modeling multiple ecosystem services, biodiversity conservation, commodity production, and tradeoffs at landscape scales. *Frontiers in Ecology and the Environment*, *7*(1), 4–11. DOI: 10.1890/080023

Nilsson, C., Reidy, C. A., Dynesius, M., & Revenga, C. (2005). Fragmentation and flow regulation of the world's large river systems. *Science, 308*(5720), 405–8. DOI: 10.1126/science.1107887

Quintana-Rizzo, E., & Reynolds, J. E. (2010). *Regional Management Plan for the West Indian Manatee (Trichechus manatus)* (CEP Technical Report 48, UNEP). Retrieved from http://www.fws.gov/caribbean/PDF/ManateeManagementPlan.pdf

Reynolds III, J. E., Szelistowski, W. A., & León, M. A. (1995). Status and conservation of manatees *Trichechus manatus manatus* in Costa Rica. *Biological Conservation*, *71*, 193–196.

Ricciardi, A., & Rasmussen, J. B. (1999). Extinction Rates of North American Freshwater Fauna. *Conservation Biology*, *13*(5), 1220–1222. DOI: 10.1046/j.1523-1739.1999.98380.x

Ruel, J., & Ayres, M. (1999). Jensen's inequality predicts effects of environmental variation. *Trends in Ecology & Evolution, 14*(9), 361-366. DOI: 10.1016/S0169-5347(99)01664-X

Rushton, S. P., Ormerod, S. J., & Kerby, G. (2004). New paradigms for modelling species distributions? *Journal of Applied Ecology, 41*(2), 193–200. DOI: 10.1111/j.0021-8901.2004.00903.x

Schmalz, B., Kuemmerlen, M., Kiesel, J., Cai, Q., Jähnig, S. C., & Fohrer, N. (2015). Impacts of land use changes on hydrological components and macroinvertebrate distributions in the Poyang lake area. *Ecohydrology*, *8*(6), 1119–1136. DOI: 10.1002/eco.1569

Seemann, J., González, C. T., Carballo-Bolaños, R., Berry, K., Heiss, G. A., Struck, U., & Leinfelder, R. R. (2014). Assessing the ecological effects of human impacts on coral reefs in Bocas del Toro, Panama. *Environmental Monitoring and Assessment*, *186*(3), 1747–1763. DOI: 10.1007/s10661-013-3490-y

Sliva, L., & Dudley Williams, D. (2001). Buffer Zone versus Whole Catchment Approaches to Studying Land Use Impact on River Water Quality. *Water Research*, *35*(14), 3462–3472. DOI: 10.1016/S0043-1354(01)00062-8

Smethurst, D., & Nietschmann, B. (1999). The distribution of manatees (*Trichechus manatus*) in the coastal waterways of Tortuguero, Costa Rica. *Biological Conservation*, *89*(3), 267–274. DOI: 10.1016/S0006-3207(98)00154-2

Smith, K. N. (1993). *Manatee Habitat and Human-related Threats to Seagrass in Florida: A Review* (Report). Tallahassee, Florida: Department of Environmental Protection, Division of Marine Resources. Retrieved from http://myfwc.com/media/415241/manatee_habitat_human.pdf

SNE. (2016). *Plan Energético Nacional 2015-2050: Panamá, el Futuro que Queremos.* Retrieved from http://www.energia.gob.pa/tmp/file/277/plan%20energetico%20nacional%20-edicion%20ira%20-julio%202016.pdf

Solomon, B., Corey-Luse, C., & Halvorsen, K. (2004). The Florida manatee and eco-tourism: toward a safe minimum standard. *Ecological Economics, 50*(1-2), 101-115. DOI: 10.1016/j.ecolecon.2004.03.025

State of Utah Department of Environmental Quality. (2014). *Standard Operating Procedure for Turbidity Measurements Using a Turbidity Tube.* Retrieved from http://www.deq.utah.gov/Compliance/monitoring/water/docs/2014/05May/SOP_TurbidityTube_5.1.14_Rev0.pdf

STRI. (2013). *Hidrografía de Panama- Mapa y Capas*. Retrieved from http://strimaps.si.edu/portal/home/item.html?id=0707c294570d4f0e840c5b9aa5506572

Tilman, D., Fargione, J., Wolff, B., D'Antonio, C., Dobson, A., Howarth, R., … Uithol, P. W. J. (2001). Forecasting agriculturally driven global environmental change. *Science, 292*(5515), 281–284. DOI: 10.1126/science.1057544

USGS. (2009). *HYDROSHEDS: Data layers and availability*. Retrieved from https://hydrosheds.cr.usgs.gov/hydro.php

USGS. (2015). *Landsat- Earth Observation Satellites: Fact Sheet 2015-3081.* Retrieved from http://pubs.usgs.gov/fs/2015/3081/fs20153081.pdf

Wood, S. (2016). *Mixed GAM Computation Vehicle with GCV/AIC/REML Smoothness Estimation* (Package 'mgcv'). Retrieved from https://cran.r-project.org/web/packages/mgcv/index.html

Zhu, Z., & Woodcock, C. E. (2012). Object-based cloud and cloud shadow detection in Landsat imagery. *Remote Sensing of Environment, 118*, 83-94, DOI: 10.1016/j.rse.2011.10.028

Zhu, Z., Wang, S., and Woodcock, C. E. (2015). Improvement and Expansion of the Fmask Algorithm: Cloud, Cloud Shadow, and Snow Detection for Landsats 4-7, 8, and Sentinel 2 Images. *Remote Sensing of Environment, 159*, 269-277, DOI: 10.1016/j.rse.2014.12.014

APPENDIX

Landsat pre-processing

The coordinates selected to limit the boundaries of the Landsat imagery in the USGS Earth Explorer database are listed in Table A1. The Landsat images selected for analysis are listed in Table A2, along with the details of each that was required in the pre-processing steps in ENVI 5.3.

Table A1 Boundary coordinates for the Landsat images taken to cover the entirety of the Changuinola River watershed in Bocas del Toro, Panama.

Point	Latitude	Longitude
1	09°43’42”N	082°03’29”W
2	09°43’42”N	083°11’03”W
3	08°45’09”N	083°11’03”W
4	08°45’09”N	082°03’29”W

Table A2 Landsat images selected between 2000 and 2015 to illustrate land use in the Changuinola watershed over time. All were downloaded in the UTM17N_WGS84 coordinate system, with 30m resolution from the USGS.

Landsat Scene ID	Sensor	Date	Time	Cloud cover (%)	Path	Row
LC80140542015126LGN00	L8 OLI	2015-05-06	15:47:45	15.32	14	54
LC80140542014027LGN00	L8 OLI	2014-01-27	15:49:44	3.74	14	54
LT50140542011051CHM00	Landsat TM (5)	2011-02-20	15:38:36	16	14	54
LE70140532007112ASN00	Landsat 7 ETM+ (SLC off)	2007-04-22	15:38:43	4	14	53
LE70140542006013EDC00	Landsat 7 ETM+ (SLC off)	2006-01-13	15:38:30	7	14	54
LE70140542003021EDC00	Landsat 7 ETM+ (SLC on)	2003-01-21	15:37:07	17	14	54
LT50140542000357AAA02	Landsat TM (5)	2000-12-22	15:28:15	0	14	54

Radiometric calibration settings were set to create a radiance band Interleaved by Line (BIL) float image with a scale factor of 0.1. To determine the atmospheric correction settings for the FLAASH tool, the Google Earth path and elevation tools were used to roughly estimate the approximate elevation of the area (elevation is only specified to the nearest kilometer in the tool, thus the values provided by Google Earth were more than sufficiently accurate to parameterize the model), which was inputted as an average elevation of 1.127km. A “Tropical” atmospheric model and “Rural” aerosol model were selected based on the climatic and environmental characteristics of the region. FLAASH was run with visibilities ranging from 40km to 80km, and with Aerosol Retrieval methods: standard 2-Band Kaufman-Tanre (K-T), alternative K-T, and none (Harris Geospatial Solutions, 2016).

Landsat classification

Once all images were pre-processed and corrected, they were classified using Maximum Likelihood. While these steps are described in the Methods section, the exact probabilities assigned to each land class, to adjust for similarity in spectral profiles and variance within class spectral profiles as well are listed in Table A3. An example of the similarity between the spectral signatures of a forest pixel and a non-forest pixel are illustrated in Figure A1.

Table A3 Probabilities inputted for the maximum likelihood of each supervised class in the Landsat imagery analysis.

Landsat Scene ID	Date	Forest	Non-forest Vegetation	Agriculture	Water	Soil	Urban
LC80140542015126LGN00	2015-05-06	0.1	0.05	0.4	0	0	0.6
LC80140542014027LGN00	2014-01-27	0.05	0.05	0.5	0.01	0.05	0.6
LT50140542011051CHM00	2011-02-20	0.1	0.1	0.5	0.05	0.05	0.6
LE70140532007112ASN00	2007-04-22	0.1	0.05	0.4	0.01	0.05	0.6
LE70140542006013EDC00	2006-01-13	0.05	0.1	0.4	0.3	0.05	0.6
LE70140542003021EDC00	2003-01-21	0.05	0.05	0.4	0.01	0.05	0.6
LT50140542000357AAA02	2000-12-22	0.05	0.1	0.4	0.05	0.05	0.6

a) Forest

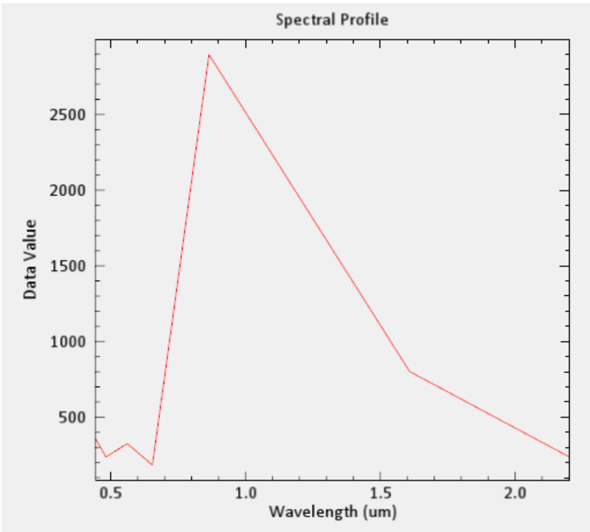

b) Non-forest

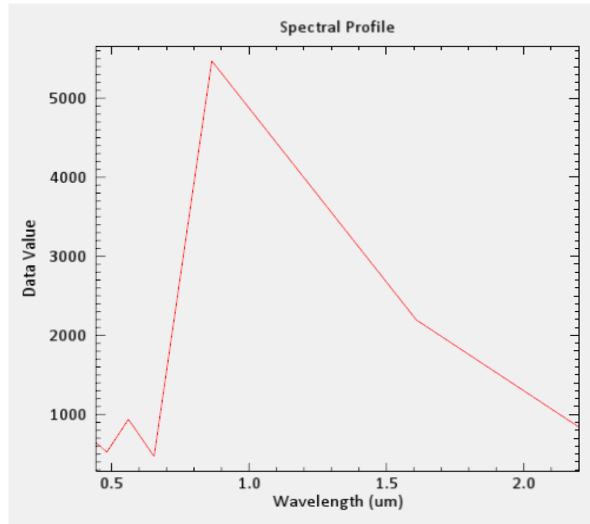

Figure A1 Example spectral signatures of the 6 land use classes identified in the Changuinola River watershed. The units of the "Date Value" variable are in reflectance, scaled by 10,000 in the FLAASH tool in ENVI 5.3.

The final step of the classification was to combine all images selected in the BULC tool. Because a base map was required to provide a base for the program to estimate pixel values, GlobCover 2009 was inputted into the model and translated into the land use classes used in this analysis. The translation of the GlobCover 2009 classes into the six land use classes of this study are demonstrated in Table A4.

Table A4 Reclassification of GlobCover (GC) 2009 classes to current study's classification system (ESA, 2010).

GC Value	GC Class	Reclassified
11	Post-flooding or irrigated croplands (or aquatic)	Agriculture
14	Rain-fed croplands	Agriculture
20	Mosaic cropland (50-70%) / vegetation (grassland/shrub land/forest) (20-50%)	Agriculture
30	Mosaic vegetation (grassland/shrub land/forest) (50-70%) / cropland (20-50%)	Non-forest vegetation
40	Closed to open (>15%) broad-leaved evergreen or semi-deciduous forest (>5m)	Forest
50	Closed (>40%) broad-leaved deciduous forest (>5m)	Forest
60	Open (15-40%) broad-leaved deciduous forest/woodland (>5m)	Forest
70	Closed (>40%) needle-leaved evergreen forest (>5m)	Forest
90	Open (15-40%) needle-leaved deciduous or evergreen forest (>5m)	Forest
100	Closed to open (>15%) mixed broad-leaved and needle-leaved forest (>5m)	Forest
110	Mosaic forest or shrub land (50-70%) / grassland (20-50%)	Forest
120	Mosaic grassland (50-70%) / forest or shrub land (20-50%)	Non-forest vegetation
130	Closed to open (>15%) (broad-leaved or needle-leaved, evergreen or deciduous) shrub land (<5m)	Forest

140	Closed to open (>15%) herbaceous vegetation (grassland, savannas or lichens/mosses)	Non-forest vegetation
150	Sparse (<15%) vegetation	Non-forest vegetation
160	Closed to open (>15%) broad-leaved forest regularly flooded (semi-permanently or temporarily) - fresh or brackish water	Water
170	Closed (>40%) broad-leaved forest or shrub land permanently flooded - saline or brackish water	Water
180	Closed to open (>15%) grassland or woody vegetation on regularly flooded or waterlogged soil - fresh, brackish or saline water	Water
190	Artificial surfaces and associated areas (urban areas >50%)	Urban
200	Bare areas	Soil
210	Water bodies	Water
220	Permanent snow and ice	Water
230	No data (burnt areas, clouds)	No Data

Predictor variables and Pearson correlation

Table A5 Pearson correlation values between predictor variables in the PA model.

	Soil	Forest	Agriculture	Non-forest	Urban	Depth	Salinity	Turbidity	Width	Slope	Feeding
Soil	1	0.0657	-0.1237	-0.0918	-0.1368	0.1405	0.1976	-0.0093	-0.0219	0.0831	0.0213
Forest	0.0657	1	-0.5455	-0.2245	-0.6745	0.1001	-0.0086	-0.3663	-0.0125	0.0955	-0.0133
Agriculture	-0.1237	-0.5455	1	-0.0241	0.6333	-0.1102	-0.1623	0.1824	-0.2756	-0.2668	0.0557
Non-forest	-0.0918	-0.2245	-0.0241	1	-0.1739	0.1105	-0.2268	-0.126	0.5587	0.1929	-0.2216
Urban	-0.1368	-0.6745	0.6333	-0.1739	1	-0.1449	-0.0846	0.3181	-0.3669	-0.2286	0.2502
Depth	0.1405	0.1001	-0.1102	0.1105	-0.1449	1	0.3807	0.07	0.2411	0.1684	0.2139
Salinity	0.1976	-0.0086	-0.1623	-0.2268	-0.0846	0.3807	1	-0.0525	0.1024	0.0503	-0.0808
Turbidity	-0.0093	-0.3663	0.1824	-0.126	0.3181	0.07	-0.0525	1	-0.1942	-0.0694	0.1381
Width	-0.0219	-0.0125	-0.2756	0.5587	-0.3669	0.2411	0.1024	-0.1942	1	0.1748	-0.1585
Slope	0.0831	0.0955	-0.2668	0.1929	-0.2286	0.1684	0.0503	-0.0694	0.1748	1	0.0321
Feeding	0.0213	-0.0133	0.0557	-0.2216	0.2502	0.2139	-0.0808	0.1381	-0.1585	0.0321	1

Table A6 Pearson correlation values between predictor variables in the FA model.

	Soil	Forest	Agriculture	Non-forest	Urban	Depth	Salinity	Turbidity	Width	Slope	Feeding
Soil	1	0.0551	0.0511	0.1313	-0.0560	-0.1933	-0.1650	-0.3163	0.3212	0.0670	0.2250
Forest	0.0551	1	0.2550	-0.0937	0.1081	0.2054	0.0836	0.0760	-0.2326	-0.1320	-0.0790
Agriculture	0.0511	0.2550	1	-0.1648	0.5467	0.2972	0.0853	0.3259	-0.2661	0.4076	-0.2888
Non-forest	0.1313	-0.0937	-0.1648	1	-0.1996	-0.2439	-0.2930	-0.3589	0.1088	-0.1828	0.2891
Urban	-0.0560	0.1081	0.5467	-0.1996	1	0.0906	-0.1811	0.2955	-0.0974	0.5088	-0.3423
Depth	-0.1933	0.2054	0.2972	-0.2439	0.0906	1	0.2373	0.3057	-0.3037	0.1135	-0.2178
Salinity	-0.1650	0.0836	0.0853	-0.2930	-0.1811	0.2373	1	0.2040	-0.4753	0.0343	-0.0668
Turbidity	-0.3163	0.0760	0.3259	-0.3589	0.2955	0.3057	0.2040	1	-0.8246	-0.0561	-0.6505
Width	0.3212	-0.2326	-0.2661	0.1088	-0.0974	-0.3037	-0.4753	-0.8246	1	0.2681	0.6753
Slope	0.0670	-0.1320	0.4076	-0.1828	0.5088	0.1135	0.0343	-0.0561	0.2681	1	0.2921
Feeding	0.2250	-0.0790	-0.2888	0.2891	-0.3423	-0.2178	-0.0668	-0.6505	0.6753	0.2921	1

Monthly discharge on gauged channels

Table A7 Mean monthly discharge (m^3/s) at each ETESA gauge (ETESA, n.d.).

Month	Station 910102	Station 910401	Station 910202
1	220.01	17.94	84.90
2	191.42	11.23	49.50
3	149.04	13.10	42.95
4	126.13	14.93	36.20
5	201.06	16.76	62.63
6	196.61	20.41	66.58
7	181.23	30.54	63.64
8	191.94	42.76	63.46
9	187.20	17.50	67.48
10	189.54	16.23	73.47
11	250.32	28.11	101.85
12	234.91	22.99	89.88

Estimated monthly discharge rates

Table A8 Mean monthly discharge rates (m^3/s) in 2015 at the Changuinola I dam, Panama without (AES Changuinola, personal communication, Mar. 21, 2016) and with the dam present, and the same at the study site downstream (calculated from Equations 2 and 3, respectively).

Month	Changuinola I Dam	Changuinola I Dam (natural)	Site	Site (natural)
1	154.64	162.24	420.85	428.46
2	143.2	141.16	338.94	336.9
3	105.39	109.91	263.92	268.44
4	70.33	93.01	210.12	232.8
5	134.63	148.28	359.39	373.04
6	187.93	144.99	421.41	378.47
7	212.74	133.65	443.17	364.09
8	126.85	141.55	381.01	395.7
9	98.41	138.05	321.77	361.41
10	101.61	139.78	329.98	368.15
11	134.69	184.6	457.38	507.29
12	118.52	173.24	405.5	460.22
Sum	**1588.94**	**1710.46**	**4353.44**	**4474.97**